Journal of Alzheimer's Disease 32 (2012) 57–76
DOI 10.3233/JAD-2012-120406
IOS Press

Parkin Null Cortical Neuronal/Glial Cultures are Resistant to Amyloid-$\beta_{1\text{-}42}$ Toxicity: A Role for Autophagy?

Rosa M. Solano[a,1], Maria J. Casarejos[a,1], Ana Gómez[a], Juan Perucho[a], Justo García de Yébenes[b] and Maria A. Mena[a,*]
[a]*Department of Neurobiology, Hospital Ramón y Cajal and Centro de Investigación Biomédica en red sobre Enfermedades Neurodegenerativas (CIBERNED), Madrid, Spain*
[b]*Department of Neurology, Hospital Ramón y Cajal and Centro de Investigación Biomédica en red sobre Enfermedades Neurodegenerativas (CIBERNED), Madrid, Spain*

Accepted 22 May 2012

Abstract. Dementia occurs often in late stages of Parkinson's disease (PD) but its cause is unknown. Likewise there is little information about the interaction between proteins that produce PD and those implicated in Alzheimer's disease (AD). Here we have investigated the interactions between parkin protein and the amyloid-β $(A\beta)_{1\text{-}42}$ peptide. We examined the effects of oligomeric $A\beta_{1\text{-}42}$ peptide on the survival, differentiation, and signaling pathways in cortical cultures from wild type (WT) and parkin null (PK-KO) mice. We discovered that PK-KO cells were more resistant than WT to $A\beta_{1\text{-}42}$. This peptide induced neuronal cell death, astrogliosis, microglial proliferation, and increased total and hyperphosphorylated tau and levels of chaperones HSP-70 and CHIP in WT, but not in Aβ-treated PK-KO cultures. $A\beta_{1\text{-}42}$ decreased proteasome activities in WT and PK-KO cultures, but the ubiquitination of proteins only increased in WT cultures. $A\beta_{1\text{-}42}$ induced a short activation of ERK1/2 and AKT signaling pathways, implicated in cell survival, in PK-KO-treated cells, and a shift in the autophagy marker LC3-II/LC3-I ratio. In addition, the percentage of cells immunoreactive to both HSC70 and LAMP-2A increased in PK-KO cultures versus WT and furthermore in PK-KO cultures treated with $A\beta_{1\text{-}42}$. Pre-treatment with inhibitors of glutathione synthesis or autophagy reverted the resistance to $A\beta_{1\text{-}42}$ of the PK-KO cultures. In conclusion, the loss of parkin protein triggers the compensatory mechanisms of cell protection against $A\beta_{1\text{-}42}$. Parkin suppression, therefore, is not a risk factor for dementia of AD type.

Keywords: Alzheimer's disease, apoptosis, autophagy-lysosomal pathway, chaperones, cortical neuron/glial cultures, glutathione, Park 2 gene, ubiquitin proteasome system

Supplementary data available online: http://dx.doi.org/10.3233/JAD-2012-120406

INTRODUCTION

There is a great interest in the mechanisms which control the production, metabolism, processing, and elimination of the amyloid-β (Aβ) peptides, since these peptides are considered responsible for the formation of plaques and aggregates which ultimately leads to synaptic loss, neuronal death, and Alzheimer's disease (AD) pathology. Previous studies, including some from our laboratory, have indicated that the processing and elimination of Aβ peptides is modulated by a great number of genetic modifiers [1–8], as well as by neuronal compounds [9–13] and pharmaceutical agents [14–18]. Among the genetic modifiers, the apolipoprotein E4 (ApoE4) allele is known to aggravate Aβ pathology [19, 20], and the ApoE2 is known to reduce the risk of AD [21]. Finally, recent

[1]These authors contributed equally to this work.

*Correspondence to: Dr. M.A. Mena, Dpto. Neurobiología-Investigación, Hospital Ramón y Cajal, Ctra. de Colmenar, Km. 9, Madrid 28034, Spain. Tel.: +34 91 336 83 84; Fax: +34 91 336 90 16; E-mail: maria.a.mena@hrc.es.

ISSN 1387-2877/12/$27.50

findings obtained using synthetic Aβ peptides and human samples indicated that low-n oligomers (from dimmers to octamers) may be proximate toxins for neuron and synapse [22–25].

We have previously shown, in *ex vivo* experiments, that the abnormal cognitive parameters, the increased risk of death, the abnormal neurochemical abnormalities and the amyloid and tau pathology observed in transgenic mice, bearing the $A\beta PP_{swe}$ mutation, which in humans produce early onset amyloidal AD, are reduced in $A\beta PP_{swe}$ mice in which the parkin protein has been completely suppressed or reduced to 50% [2].

Parkin protein is an ubiquitin E3 ligase involved in the ubiquitin-proteasome system (UPS) of processing abnormal protein [26–33]. The suppression of parkin, therefore, was expected to interfere with the elimination of abnormal protein and to increase the accumulation of Aβ peptide and the AD pathology. We discovered, however, that the amelioration of Aβ pathology induced by parkin suppression was related to compensatory hyperactivation of other alternative mechanisms of protein elimination, namely macroautophagy and chaperone mediated autophagy (CMA) [2].

Here, we investigate whether the compensatory mechanism present in neuronal cells from parkin null mice (PK-KO) could prevent the neurotoxic effects of the oligomeric form of $A\beta_{1\text{-}42}$ peptide added to the cultures of PK-KO in comparison with those observed in neuronal cultures from wild type (WT) treated with $A\beta_{1\text{-}42}$ peptide. These set of new experiments investigate the role of parkin on an acute overload of $A\beta_{1\text{-}42}$ peptide, a very different setting from our experiments performed in $A\beta PP_{swe}$ mice with full, hemizygotic, or null parkin expression. We have also studied the molecular mechanisms involved in the processing of the toxic $A\beta_{1\text{-}42}$ peptide with pharmacological tools which allow for the evaluation of the role of this mechanism in the processing of toxic amyloid peptides.

MATERIALS AND METHODS

Culture media and chemicals

Dulbecco's modified Eagle's medium (DMEM) with high glucose (4.5 g/L), Ham's F12 nutrient mixture, Eagle's minimal essential medium (EMEM) with Earl's salts, Leibovitz's L-15 medium, B27/Neurobasal TM medium, Hank's balanced salt solution, L-glutamine, pyruvate, penicillin-streptomycin, and fetal bovine serum (USA origin) were purchased from Gibco-Life Technologies (Paisley, Scotland, UK). Glucose 45%, Trypsin-EDTA, insulin, putrescine, progesterone, sodium selenite, and poly-D-lysine were from Sigma (Madrid, Spain) and human transferrin, 30% iron-saturated, from Boehringer-Mannheim (Barcelona, Spain). Bovine serum albumin (BSA), bis-benzimide, L-buthionine-[S,R]-sulfoximine (BSO), and 3-methyladenine (3MA) were from Sigma (Madrid, Spain). Laminin was from Roche (Barcelona, Spain). The cytotoxicity detection kit for LDH was from Boehringer-Mannheim (Barcelona, Spain). $A\beta_{1\text{-}42}$ peptide was from (Bachem, Switzerland) and the BCA protein assay kit was from Pierce (Rockford, IL, USA). All other reagents were of the highest purity commercially available from Merck or Sigma.

Cell cultures

Neuronal-enriched, neuron-glia and glial cortical cultures were obtained from 129SV/C57BL/6 WT or parkin mutant mice (PK-KO) [34]. Cultures were derived from littermate –/– and +/+ embryos obtained from homozygous colonies previously generated by heterozygous parkin −/+ intercross. The genotype was confirmed by standard PCR techniques of genomic DNA obtained from their tails [35, 36]. Procedures using laboratory animals were in accordance with the European Union Directives and the Ramón y Cajal University Hospital Animal Care Committee. All efforts were made to minimize the number of animals used and their suffering. Neuronal-enriched, mixed neuron-glia, and glial cultures were prepared from cortical tissues of embryonic day 15/16 mice; a previously described method for making neuron-enriched or glial cultures of E13 mesencephalic tissue was adapted to this purpose [36, 37].

For neuron-glia primary cultures, cortical tissues were obtained from embryonic tissue (16th day gestation), incubated with 0.36 mg/ml papain in PBS/D-glucose (6 mg/ml)/1% BSA buffer for 15 min at 37°C and mechanically dissociated in presence of 10 mg/ml Dnase-I. The cells were seeded in B27/Neurobasal TM medium with 15% (v/v) heat-inactivated fetal calf serum (B27/NBL-FCS) supplemented with glutamine (4 mM), penicillin (100 U/ml), and streptomycin (100 μg/ml) in multiwells or in glass cover slides pre-coated with poly-D-lysine (4.5 $\mu g/cm^2$) in 0.1 M borate buffer, pH = 8.4 and laminin (3 μg/ml). The cultures were kept in a humidified chamber at 37°C in a 5% CO_2 atmosphere for 7-8 days *in vitro* (DIV). Neurons were easily distinguishable from glia: they appeared phase-bright,

had smooth, rounded somata and distinct processes, and lay just above the focal plane of the glial layer. Cells were treated at 5-6 DIV unless stated otherwise.

For glial cultures, the cortices were removed from embryonic tissue (16th day gestation), diced in small fragments, and incubated in trypsin-EDTA (0.5% in Hank's balanced salt solution) at 37°C for 15 min. Trypsinization was stopped by adding culture medium, and the tissue was gently centrifuged. The supernatant was discarded, and the pellet resuspended in 1 ml of culture medium. Single cell dissociation was achieved by mechanical disruption. Dissociated cells were plated in DMEM with 15% (v/v) heat inactivated fetal bovine serum, 4 mM L-glutamine, 1 mM pyruvate, and 100 U/ml penicillin-streptomycin (growth medium; DMEM-FCS) [38] at a density of 3×10^6 cells per 80-cm^2 cell culture flasks. Culture medium was refreshed after 6-7 days and every 7 days thereafter. After 20 days in culture, positive staining with anti-GFAP antibody identified the astrocytes in these cultures and contained at least 80–90% of total cells.

For neuronal-enriched cultures, the cortices were removed from embryonic tissue (16th day gestation) and incubated with 0.36 mg/ml papain in PBS/D-glucose (6 mg/ml)/1% BSA buffer for 15 min at 37°C and mechanically dissociated in presence of 10 mg/ml Dnase-I. The cells were seeded in B27/Neurobasal TM medium with 15% (v/v) heat inactivated fetal calf serum (B27/NBL-FCS) supplemented with glutamine (4 mM), penicillin-streptomycin (100 U/ml) at a density of 2.5×10^5 cells/cm^2 in multiwells or 2×10^5 cells/cm^2 in glass cover slides pre-coated with poly-D-lysine (4.5 μg/cm^2) in 0.1 M borate buffer, pH = 8.4 and laminin (3 μg/ml). The cultures were kept in a humidified chamber at 37°C in a 5% CO_2 atmosphere for 7-8 DIV. Twenty-four hours after plating, the cells were changed to serum-free medium (B27/NBL).

Preparation of Aβ peptide

Aβ oligomers: synthetic $A\beta_{1\text{-}42}$ (Bachem) peptide was dissolved in 1,1,1,3,3,3-hexafluoro-2-propanol (HFIP) to 1 mM and aliquoted into microcentrifuge tubes, then the HFIP was evaporated, and the peptide film was stored at −80°C until use. For oligomeric assembly, concentrated peptide was resuspended in DMSO (5 mM) and then diluted to 100 μM in phenol red-free media and incubated at 4°C for 24 h. The preparation was centrifuged at $10{,}000 \times g$ for 10 min at 4°C to remove insoluble aggregates, and the supernatant containing soluble oligomers was transferred to clean tubes and used for the treatment of neuron-glia or glial cultures. 0.5 μg were loaded to 15% SDS-PAGE gels and detected after western blot analysis with mouse monoclonal Aβ antibody 6E10 to demonstrate the presence of soluble oligomeric forms of Aβ (Fig. 1A).

Treatment of neuronal-enriched, neuron-glia, and glial cortical cultures

For neuron-glia cultures, before the $A\beta_{1\text{-}42}$ oligomers treatment, the cells were changed to serum-free defined Neurobasal medium containing 2% B27 supplement without antioxidant (Invitrogen). The cultures (neuronal-enriched and neuron-glia cortical cultures), maintained for 7-8 DIV, were seeded with a density of 4×10^5 cell/ml in 24, 12, or 6-well plate cultures, and 150,000 cells in cover-slides for immunocytochemistry (ICQ) studies. For curve-dose response experiments, the cultures were treated with oligomeric $A\beta_{1\text{-}42}$ (0.55; 1.1; 2.2; or 4.4 μM) for 48 h and then, cell viability studies were made. To study the cell phenotype affected by $A\beta_{1\text{-}42}$ treatment (4.4 μM for 48 h) ICQ studies were performed.

To test the role of glutathione (GSH) and autophagy in the different response to $A\beta_{1\text{-}42}$ from WT and PK-KO cultures, we used the GSH synthesis inhibitor (0.75 μM) 30 min before $A\beta_{1\text{-}42}$ (4.4 μM for 48 h), and the autophagy inhibitor 3-methyladenine (3-MA, 0.5 mM, 30 min before the $A\beta_{1\text{-}42}$ treatment).

For western blot and proteasome activity experiments, neuron-glia cultures seeded in 12 and 6- well plates, respectively were treated for 48 h with vehicle or $A\beta_{1\text{-}42}$ at 4.4 μM.

Glial cell treatments

After 15–20 DIV in growth medium (DMEM-FCS), glial cultures had reached confluence; at this time, the cells were mildly trypsinized and reseeded for the different experiments at a density of 1.5×10^4 cells/cm^2 in 12-well cultures plates and maintained in growth medium for 5-6 additional days. To study the effect of $A\beta_{1\text{-}42}$ in cell viability after 5-6 days of re-seeding, the culture medium was changed to serum-free defined medium (EF12) and the cells treated with $A\beta_{1\text{-}42}$ at 4.4 μm for 48 h. Western blot experiments were conducted to detect ERK1/2- and AKT-phosphorylation time curse profile.

Cell viability measurements

Apoptosis was measured by light microscopy features and DNA staining. Cells growing on cover slides

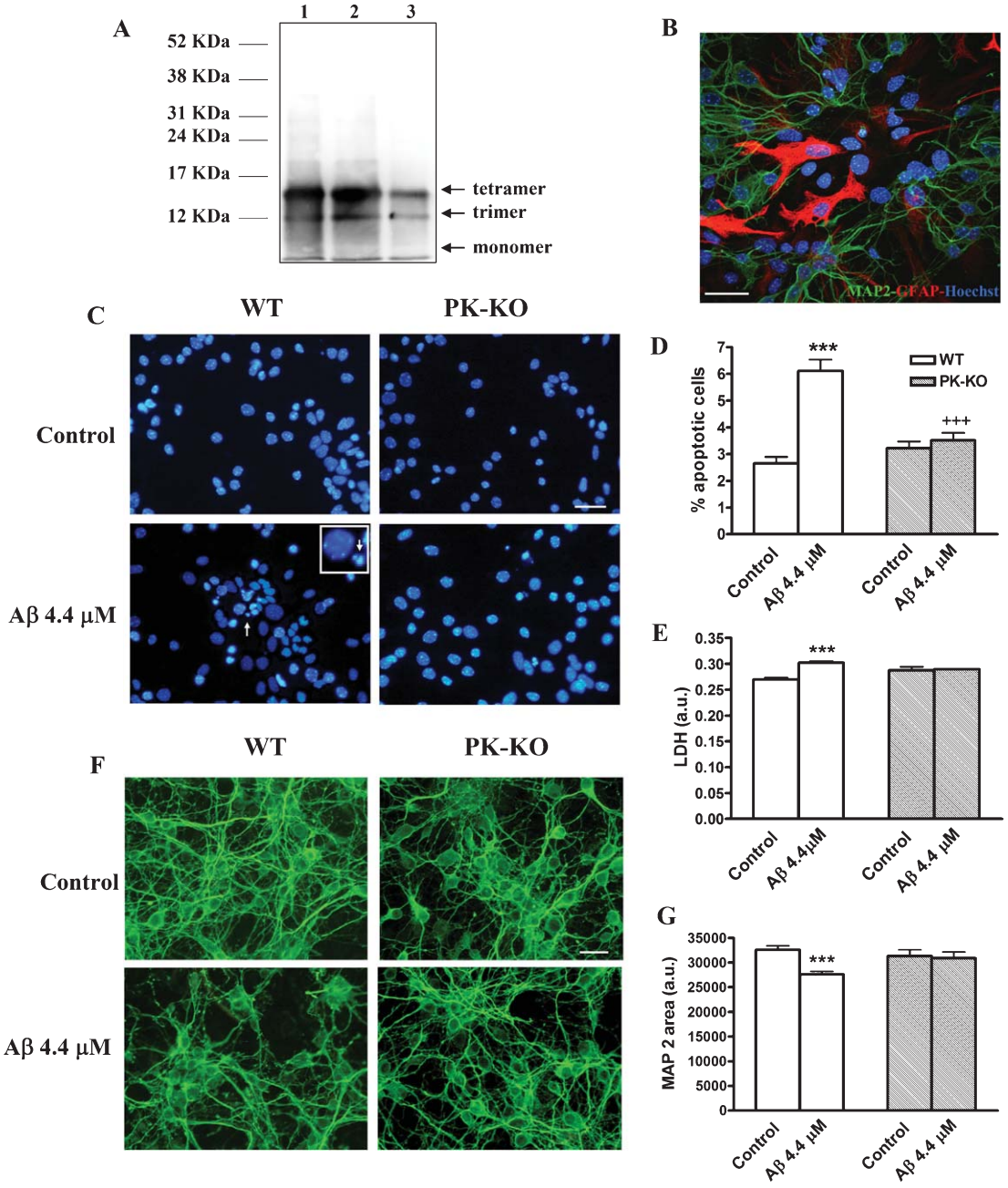

Fig. 1. PK-KO neuron-glia cultures were resistant to oligomeric form of $A\beta_{1\text{-}42}$. A) Aggregation state of $A\beta_{1\text{-}42}$ in three preparations used for the experiments. Representative western blot analysis show the presence of soluble oligomers (monomers, trimers, and tetramers) in the samples. B) Photomicrograph of neuron-glia cortical culture from PK-KO, staining neurons ($MAP2^+$), type 2 astrocytes ($GFAP^+$), and nuclei (bis-benzimide). Scale bar, 30 μm. After 5 days *in vitro*, the cultures were treated with $A\beta_{1\text{-}42}$ at 4.4 μM for 48 h. C) Photomicrographs of total nuclei stained with bis-benzimide. Inset showing peripheral chromatin-condensed nuclei. D) Percentage of apoptotic cells with respect to the total cell number in WT and PK-KO mixed cultures treated with $A\beta_{1\text{-}42}$ or solvent. E) LDH activity in the medium of WT and PK-KO mixed cultures treated or untreated with the amyloid. F) Photomicrographs and (G) quantification of total neurons ($MAP2^+$ cells) in WT and PK-KO cultures from control and $A\beta_{1\text{-}42}$ treated cells. Scale bar, 30 μm. Values are the mean ± SEM from two independent experiments with 4–6 replicates each. Statistical analysis was performed by one or two-way ANOVA followed by Newman Keuls multiple comparison test and Bonferroni post-test, respectively. $^{***}p < 0.001$ Aβ treated cultures versus their respective controls; $^{+++}p < 0.001$ PK-KO versus WT cultures. The interaction between the genotype and the treatment was $F(1,66) = 24.89$; $p < 0.0001$ for C. $F(1,24) = 17.01$; $p = 0.0013$ for D and $F(1,24) = 0.069$; $p = 0.069$ for F.

were fixed in 4% paraformaldehyde, and the nuclei were stained with bis-benzimide (Hoechst 33342) added to the anti-fading solution, 3×10^{-6} M final concentration [39, 40], and counted in 1/14 of the cover slide area; apoptotic cells were identified by chromatin condensation and fragmentation.

Mitochondrial activity was measured with the 3-(4,5-dimethyl-thiazol-2-yl)-2,5 diphenyltetrazolium bromide assay, which measures the metabolism of 3-(4,5-dimethylthiazol-2-yl)-2,5-diphenyl tetrazolium bromide.

For necrotic cell death determination, lactate dehydrogenase (LDH) activity was performed. LDH was measured in the culture medium by using a cytotoxicity detection kit [36, 37].

Immunocytochemistry

Cortical neurons were stained with an antibody against microtubule-associated protein-2 (MAP-2) (Sigma, Madrid, Spain), a marker for the cell body and neurite, diluted at 1 : 200, and astrocytes with a rabbit anti-GFAP antibody (1 : 500) from DAKO (Glostrup, Denmark). Microglial cells were identified with isolectin B_4 peroxidase-labeled (12.5 μg/ml) (Sigma, Madrid, Spain) [41, 42]. Caspase-3 activation was stained with a rabbit polyclonal anti-cleaved caspase-3 (1 : 400) from Cell-Signaling Technology (Boston, MA, USA).

We analyzed the percentage of cells immunoreactive to both HSC70 and LAMP-2A as markers of chaperon-mediated autophagy [43, 44]. Mouse anti-HSC70 diluted 1/100 and rabbit anti-LAMP-2A diluted 1/100 were from Abcam (Cambridge, UK). Colocalization images for HSC70 and LAMP-2A were acquired using a Nikon C1 plus ECLIPSE Ti-e microscope and a 60X Plan Apo VC oil objective with NA 1.4 laser-scanning confocal microscope.

The cell cultures were fixed with 4% paraformaldehyde, washed in 0.1 M phosphate-buffered saline, pH 7.4 (PBS), permeabilized with ethanol-acetic acid (19 : 1), and incubated at 4°C for 24 h with primary antibodies diluted in PBS containing 10% fetal calf serum. Fluorescein- and rhodamine-conjugated secondary antibodies (Jackson ImmunoResearch, West Grove, PA, USA) were employed to visualize positive cells under fluorescent microscopy. For microglial cells identification, cultures were fixed with 4% paraformaldehyde +1% glutaraldehyde and incubated at 4°C for 24 h with isolectin B_4 peroxidase-labeled diluted in TBS/0.1% triton X-100; the positive cells were developed with a DAB-system (LSAB2 system, DAKO) and visualized under optical microscopy.

The number of immunoreactive cells was counted in one-seventh of the total area of the cover slides. The cells were counted in predefined parallel strips using a counting reticule inserted into the ocular.

The intensity and the area of fluorescence of GFAP and MAP-2 immunostaining were measured in 20 pre-defined fields for each slide, processed with the automatic software Image-Pro 6.2 (Media Cybernetics, Silver Spring, MD, USA) and expressed as arbitrary units or intensity (integrated optical density). For all immunocytochemical methods, negative controls were tested by incubation without the primary antibody in each case.

Measurement of glutathione levels and glutathione peroxidase activity

Total GSH levels were measured as previously described [45]. Briefly, the cells from neuron-glia cultures were washed with PBS, lysed in 100 μl of 0.4 N perchloric acid (PCA) for 30 min at 4°C, and centrifuged, and the supernatants were neutralized with four volumes of 0.1 M NaH_2PO_4, 5 mM EDTA, pH 7.5. GSH content was measured in a P96 automatic reader by the addition of 5,5′-dithio-bis-2-nitrobenzoic acid (DTNB, 0.6 mM), nicotinamide adenine dinucleotide phosphate reduced tetrasodium salt (NADPH, 0.2 mM), and glutathione reductase (1 U). The reaction was monitored at 412 nm for 6 min.

In WT and PK-KO neuron-glial cultures after 7 DIV, the cells were washed with PBS, harvested by centrifugation at 1000 × g for 5 min, pooled in 110 μl of 50 mM potassium phosphate (pH 7.2), 1 mM EDTA and sonicated. The homogenate was centrifuged at 10.000 × g for 15 min at 4°C, and the supernatant was used for glutathione peroxidase (GPx) and protein determination. GPx activity was measured according to the method of Flohe and Gunzler [46]. Briefly, 110 μl of 50 mM potassium phosphate pH 7.2, 1 mM EDTA, 25 μl of 10 mM GSH and 25 μl of GSH reductase (0.6 U/μl) were added over 40 μl of the cell homogenates. This reaction mixture was incubated for 5 min at 37°C after which 25 μl of 1.5 mM NADPH was added. The change in absorbance was followed at 340 nm for 5 min at room temperature in order to quantify the hydroperoxide independent oxidation of NADPH. 25 μl of 12 mM tert-butyl hydroperoxide were then added and the rate of NADPH oxidation was followed at 340 nm for 5 min. One unit of GPx activity is the amount of enzyme necessary to oxidize 1 μmol of NADPH per minute.

Western blot analysis

Neuron-glia and glial cortical cultures were homogenized with a sonicator in lysis buffer containing 20 mM Tris HCl, 10 mM potassium acetate (AcK), 1 mM dithiothreitol (DTT), 1 mM EDTA, 1 mM PMSF, 1 mM benzamidine, leupeptin, aprotinin, pepstatin 5 μg/ml each, 0.25% NP-40, pH 7.4, and then centrifuged at 12.000 × g for 30 min at 4°C. For phospho-proteins (AKT, ERK1/2, and tau) detection, 10 mM sodium fluoride (FNa), 2 mM sodium molibdate, 10 mM β-glicerophosphate, and 0.2 mM ortovanadate were added to the lysis buffer. The supernatant was used for protein determination by the BCA protein assay kit and for electrophoretical separation. Samples (20–30 μg protein) were added to SDS sample loading buffer, electrophoresed in 10–15% SDS-polyacrylamide gels and then electroblotted to 0.45 μm nitrocellulose membranes. For immunolabeling, the blots were blocked TTBS (20 mM Tris-HCl pH 7.6, 137 mM NaCl plus 0.1% (v/v) Tween-20 and 5% dry skimmed milk) for 1 h at room temperature. After blocking non-specific binding, the membranes were incubated with different specific primary antibodies in blocking solution overnight at 4°C. The blots were developed by chemiluminiscence detection using a commercial kit (Bio-Rad) and quantified by computer-assisted videodensitometry.

The antibodies used in the study were the following: mouse monoclonal anti-beta amyloid antibody clone 6E10 (Covance, Princeton, New Jersey, USA) was used at 1 : 1000. Mouse monoclonal anti-cytochrome C (1 : 1000) was from BD Bioscience (San Jose, CA, USA). The chaperone mouse anti-HSP-70 (1 : 750), rabbit polyclonal anti-CHIP (1 : 1000), and goat polyclonal anti-p62 (SQSTM-1) (1 : 500) were from Santa Cruz (Heidelberg, Germany). Mouse monoclonal anti-tau-5 (Chemicon, Temecula, CA, USA) antibody was used at 1 : 5000 and human monoclonal anti PHF tau (AT-8) antibody (Pierce Endogen, Rockford, IL, USA) was diluted at 1 : 1000. Rabbit anti-p-GSK3α [pY^{279}]/β [pY^{216}] diluted 1/1000 and mouse anti-total GSK3 diluted 1/1000 were from Invitrogen (Carlsbad, CA, USA). Mouse monoclonal anti-ubiquitin diluted at 1 : 500 was from Chemicon, (Temecula, CA, USA). We used a mouse anti-phospho-ERK-1/2 (1 : 5000) and rabbit anti-ERK-1/2 (1 : 10000) antibodies from Sigma (Madrid, Spain). Mouse monoclonal anti-phosphorylated AKT (1 : 700); rabbit polyclonal anti-AKT (1 : 700), and rabbit polyclonal anti-PARP (1 : 1000) were from Cell-Signaling Technology (Boston, MA, USA). Rabbit polyclonal anti-LC3 antibody (MBL, Nagoya, Japan) and rabbit polyclonal anti-Beclin-1 (Sigma, Madrid, Spain) were diluted at 1 : 1000. Rabbit anti-GR diluted 1/2000, mouse anti-HSC70 diluted 1/1000 and rabbit anti-LAMP-2A diluted 1/1000 were from Abcam (Cambridge, UK). Mouse monoclonal anti-β-actin antibody (Sigma, Madrid, Spain) diluted 1 : 5000 was used as a control of charge. Goat anti-mouse, anti-rabbit, and rabbit anti-goat-HRP secondary antibodies diluted 1 : 2000 were from Sigma and Santa Cruz, respectively. β-Actin secondary antibody was an anti-mouse phosphatase alkaline conjugated diluted at 1 : 3000 from Sigma. Anti-mouse and anti-rabbit-horseradish peroxidase secondary antibodies were from Amersham and rabbit anti-goat-HRP was from Santa Cruz. β-Actin secondary antibody was an anti-mouse phosphatase alkaline conjugated (from Sigma).

Proteasomal activity measurement

After culture treatments, the cells were washed with PBS, harvested in proteasomal lysis buffer [50 mM HEPES, pH 7.5, 150 mM NaCl, 5 mM MgCl, 0.5 mM DTT (1,4-Dithiothreitol) and 0.03% triton X-100], and lysed by sonication (VibraCell, level 0.5 for 30 s). The lysates were centrifuged at 12,000 × g at 4°C for 30 min. The protein concentration was assayed from the resulting supernatants by the BCA protein assay kit. Proteasomal activities were quantified by monitoring the accumulation of the fluorescent cleavage product 7-amino-4-methylcoumarin (AMC) from the synthetic proteosomal substrates. In particular, Suc-Leu-Leu-Val-Tyr-AMC, Ac-Arg-Leu-Arg-AMC, and Z-Leu-Leu-Glu-AMC were used to measure chymotrypsin, trypsin, and peptidyl-glutamyl-peptide hydrolyzing (PGPH)-like activity of the proteasome, respectively. The assay was carried out with 25–35 μg of tissue lysates and the proteasomal substrate at 37°C for 190 min of incubation. The fluorescence of the released AMC was measured using an automatic multiwell plate reader at excitation/emission wavelengths of 360/465 nm.

Detection of ubiquitinated proteins

The neuron-glia cortical cultures were treated with Aβ1-42 at 4.4 μM or solvent for 48 h. The cells were washed with PBS plus phenylmethylsulfonyl fluoride (PMSF), scraped in 150 μl of lysis buffer [50 mM Tris HCl, 150 mM NaCl, 20 mM EDTA,

1% Triton X-100, 50 mM sodium fluoride (NaF), 20 mM N-ethyl-maleimide, 100 μM sodium ortovanadate, 1 mM PMSF, and protease inhibitors cocktail (Sigma)] and immediately boiled for 5 min. The lysates were centrifuged at 12.000 × g at 4°C for 30 min. The supernatant was used for protein determination by the BCA protein assay kit. For detection of ubiquitinated proteins by western blot, 15 μg of protein were used for electrophoretical separation in 10% of sodium dodecyl sulfate (SDS)–polyacrylamide gels.

Statistical analysis

The results were statistically evaluated for significance with one-way ANOVA followed by Newman Keuls multiple comparison test. The interactions between the genotype and the treatment were analyzed by two-way ANOVA followed by Bonferroni post-test. Differences were considered statistically significant when $p < 0.05$. Analysis of data was performed using the GraphPad PRISM 4 software.

RESULTS

Parkin knock-out neuronal-enriched, neuron-glia, and glial cortical cultures are resistant to the oligomeric form of $A\beta_{1\text{-}42}$. Patterns of cell death and phenotypes affected by the amyloid peptide treatment

We used cortical neuron-glia primary cultures to study the effects of the toxic oligomeric form of $A\beta_{1\text{-}42}$, one of the major components of amyloid pathology in AD [47]. Firstly, we characterized the cellular composition of fetal neuron-glia primary cultures from WT and parkin mutant mice grown in Neurobasal medium with 15% fetal bovine serum for 5 DIV. Immunocytochemical (Fig. 1B) analysis indicated that, at the time of treatment, the cultures contained 48.1 ± 2.66% neurons (microtubule-associated protein $2a^+$ $2b^+$), 25 ± 1.23% GFAP astrocytes, and around 2% microglial cells. The rest of the cells (23–25%) were glial progenitors (A2B5), oligodendrocytes ($O1^+$), and neuronal progenitors ($nestin^+$ cells). Neuron-glia cultures from PK-KO mice had similar proportions of the different cell types with the exception of a significant increment of microglial cells (2.1 ± 0.12% in WT versus 3.06 ± 0.21% in PK-KO) (supplementary Table 1; available online: http://www.j-alz.com/issues/32/vol32-1.html#supplementarydata01).

After performing the dose-response curve (supplementary Figure 1), we chose the treatment with $A\beta_{1\text{-}42}$ at 4.4 μM for 48 h as the optimal experimental approach for the study of the differential susceptibility of WT and PK-KO cortical cultures to $A\beta_{1\text{-}42}$ treatment. Administration of 4.4 μM of $A\beta_{1\text{-}42}$ to neuron-glia cortical cultures on 5-6 DIV for 48 h resulted in a significant cell death, as measured as the percentage of apoptotic cells (Fig. 1C, D), and the levels of LDH released into the medium (Fig. 1E). In addition, neuronal cell loss was determined by immunostaining against the neuronal cytoskeletal protein MAP2 (Fig. 1F, G) in WT neuron-glia primary cultures. In contrast, administration of $A\beta_{1\text{-}42}$ to PK-KO cultures did not induce cell death or neuronal loss (Fig. 1C–G).

Furthermore, the astroglial immunoreactivity (Fig. 2A, B), expressed as integrated optical intensity of $GFAP^+$ cells, and the percentage of microglial cells (isolectin $B4^+$ cells) (Fig. 2C, D) increased significantly in $A\beta_{1\text{-}42}$-treated neuron-glia WT cultures. PK-KO neuron-glia cultures treated with vehicle had a percentage of microglia significantly greater than the WT controls, but the treatment with $A\beta_{1\text{-}42}$, 4.4 μM, only produced a very modest increment of microglia, which did not reach significance.

PK-KO neuronal-enriched cortical cultures are resistant to $A\beta_{1\text{-}42}$ toxicity. However, in WT cultures treated with oligomeric $A\beta_{1\text{-}42}$ (4.4 μM for 48 h) a loss in the number of MAP 2 positive cells and an increase of apoptosis was observed (supplementary Figure 2).

We also used cortical glial cultures to study the effect of oligomeric $A\beta_{1\text{-}42}$ (4.4 μM for 48 h) in WT and PK-KO mice. As it happens with the neuron-glia cultures, PK-KO glial cells were more resistant than WT to the cell death induced by $A\beta_{1\text{-}42}$ (4.4 μM for 48 h) (supplementary Figure 3). Moreover, in cortical glial cultures, Aβ induced astroglial cell death and increased microglia activation in WT but not in PK-KO cultures (supplementary Figure 3F–I).

Differential effects of oligomeric $A\beta_{1\text{-}42}$ on apoptotsis, chaperones, and tau proteins

$A\beta_{1\text{-}42}$ (4.4 μM for 48 h) increased the levels of cytochrome C in WT-treated cultures, but not in PK-KO (Fig. 3A). In fact, PK-KO cultures treated with $A\beta_{1\text{-}42}$ peptide had significantly lower levels of cytochrome C than untreated WT (Fig. 3A). The Bax/Bcl2 ratio was similar in both WT and PK-KO cultures (data not shown). In addition, $A\beta_{1\text{-}42}$ (4.4 μM for 48 h) increased much more the levels of cleaved

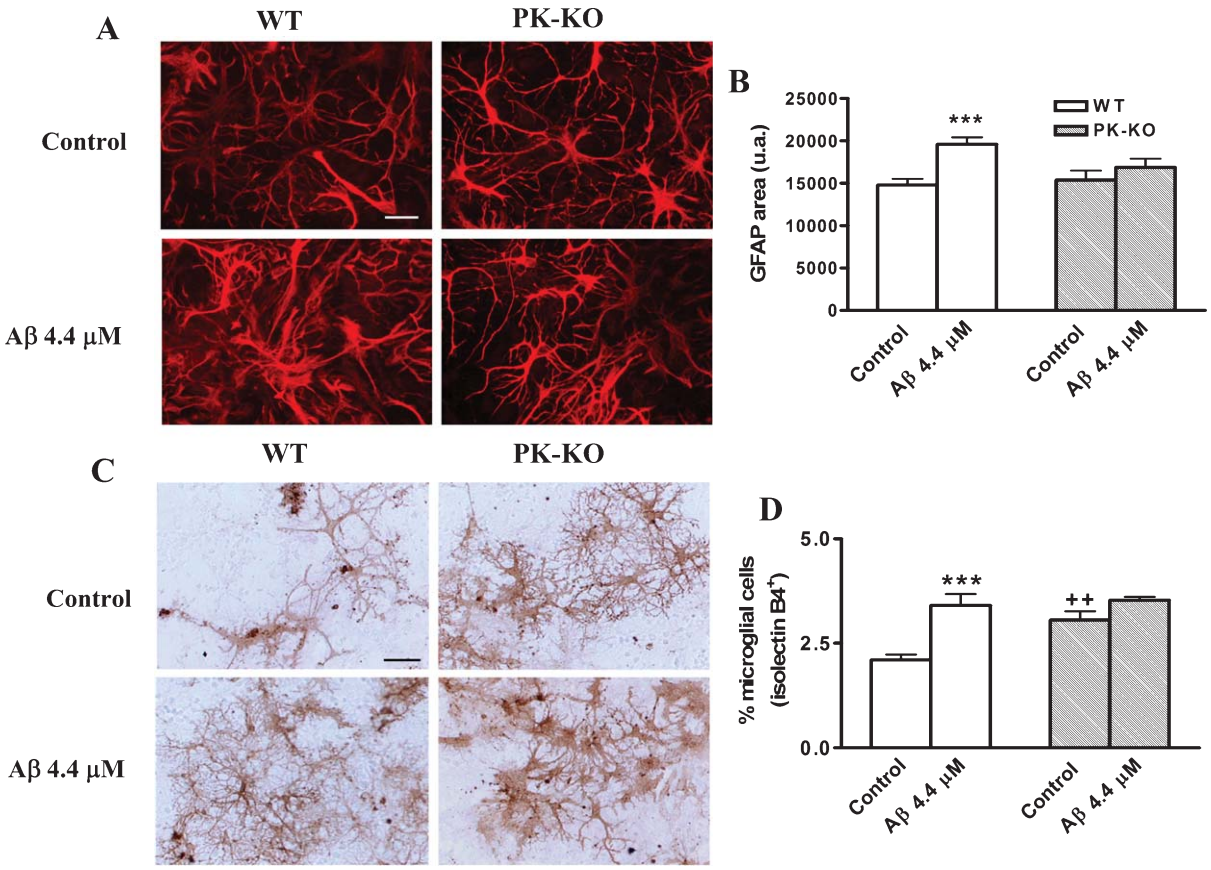

Fig. 2. Effects of oligomeric $A\beta_{1\text{-}42}$ on glial phenotypes in WT and PK-KO neuron-glia cultures. After 5 days *in vitro*, the cultures were treated with $A\beta_{1\text{-}42}$ (4.4 μM for 48 h) or solvent. A) Photomicrographs showing type 2 astrocytes ($GFAP^+$ cells) in WT and PK-KO from control and $A\beta_{1\text{-}42}$ treated cells. B) Astroglial immunoreactivity ($GFAP^+$ cells) quantification in the cultures. Photomicrographs (C) and percentage of microglial cells (D) (isolectin $B4^+$ cells) in WT and PK-KO cultures treated with $A\beta_{1\text{-}42}$ or solvent. Scale bar, 30 μm. Values are the mean ± SEM from two independent experiments with 6 replicates each. Statistical analysis was performed by one or two-way ANOVA followed by Newman Keuls multiple comparison test and Bonferroni post-test, respectively. $^{***}p < 0.001$ Aβ-treated cultures versus their respective controls, $^{++}p < 0.01$ versus WT cultures. The interaction between the genotype and the treatment was $F(1,24) = 4.65$; $p = 0.042$ for D.

nuclear poly (ADP-ribose) polymerase (PARP) in WT-treated cultures than in PK-KO-treated cells (Fig. 3B). The number of positive cells for caspase-3 active subunit increased in WT-treated cultures, but not in the PK-KO-treated (Fig. 3C, D).

HSP70 and CHIP, two chaperones upregulated in situations of stress, were further increased in WT but not in PK-KO neuron-glia primary cultures, in which the levels of the two proteins were diminished (Fig. 4A, B). Notably, PK-KO neuron-glia cultures had higher basal levels of HSP70 than WT (Fig. 4A).

Tau protein is typically hyperphosphorylated in paired helical filaments from brains of patients with AD [48], and Aβ peptides can induce *in vitro* tau phosphorylation. Therefore, we studied tau protein and their phosphorylation state in untreated and $A\beta_{1\text{-}42}$-treated WT and PK-KO neuron-glia cortical cultures. As shown in Fig. 4 C, D, the treatment of these cultures with $A\beta_{1\text{-}42}$, 4.4 μM for 48 h, increased the levels of total and phosphorylated tau protein, as detected by western blot with tau-5 and AT-8 antibodies, respectively (Fig. 4C, D), in WT but not in PK-KO cultures. There were no differences in basal levels of tau and p-tau between WT and PK-KO cultures. However, p-tau/tau-5 ratios decreased in PK-KO cultures treated with $A\beta_{1\text{-}42}$ (data no shown). In addition, p-GSK3/total GSK3 ratios increased in WT cultures treated with Aβ, but not in PK-KO treated ones (Fig. 4E).

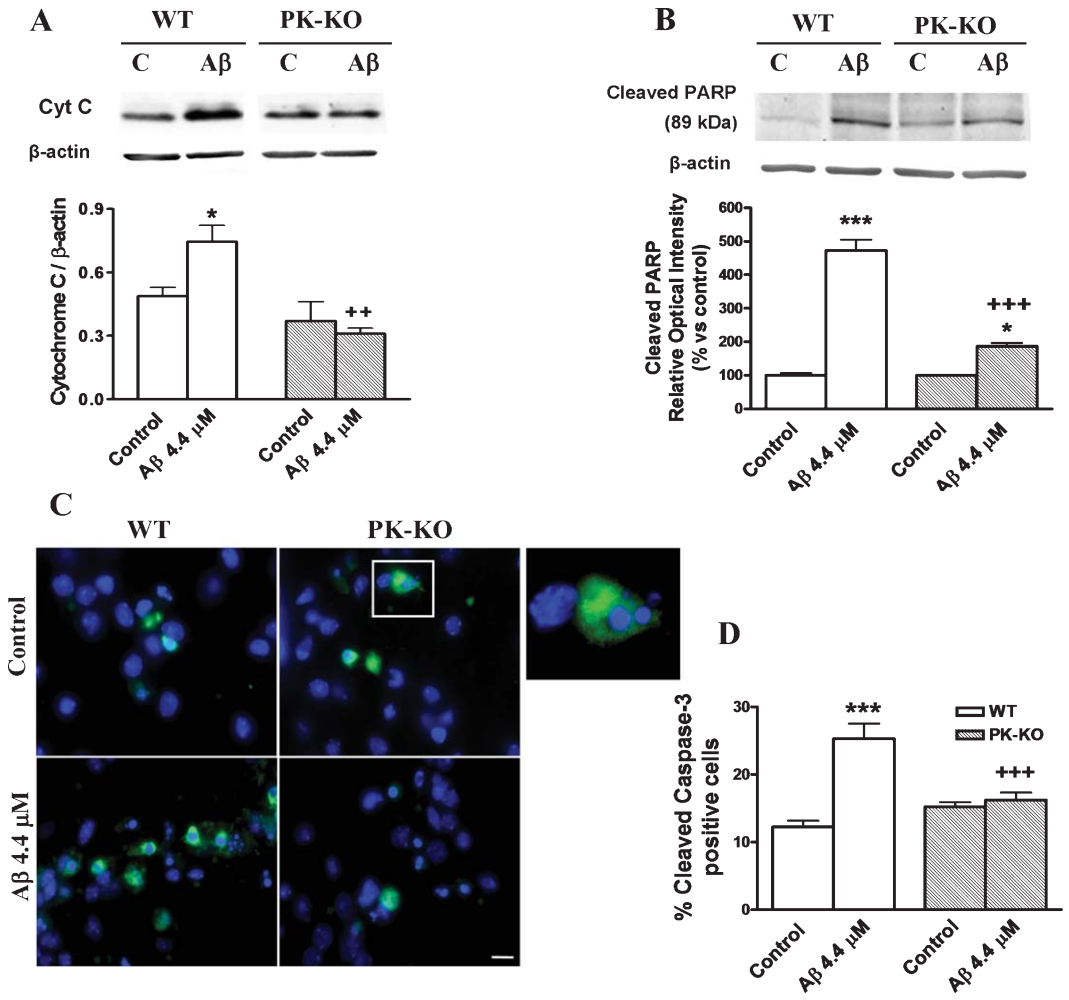

Fig. 3. Differential effects of oligomeric $A\beta_{1\text{-}42}$ on cell death in WT and PK-KO cultures. At 5 DIV WT and PK-KO neuron-glia cultures were treated with $A\beta_{1\text{-}42}$ for 48 h. A) Representative western blot and densitometric analysis of cytochrome C. B) Representative western blot and densitometric analysis of cleaved PARP protein as a marker of the final stages of apoptosis. To ensure equivalent loading of protein, both blots were reproved for β-actin. C) Micrographs of cleaved caspase-3 immunoreactive cells 48 hours after $A\beta_{1\text{-}42}$ treatment. A portion of this micrograph has been magnified in the picture of the right and (D) percentage of caspase-3 active subunit positive cells with respect to the total cell number in WT and PK-KO mixed cultures treated with $A\beta_{1\text{-}42}$ or solvent. Scale bars = 30 μm. Values are the mean ± SEM from one or two independent experiments with 4 replicates each. Statistical analysis was performed by one or two-way ANOVA followed by Newman Keuls multiple comparison test and Bonferroni post-test, respectively. $^{*}p < 0.05$, $^{***}p < 0.001$ Aβ-treated cultures versus their respective controls; $^{++}p < 0.01$, $^{+++}p < 0.001$ PK-KO versus WT cultures. The interaction between the genotype and the treatment was $F(1,25) = 6.46$; $p = 0.0176$ for A. $F(1,8) = 64.05$; $p < 0.0001$ for B and $F(1,12) = 18.48$; $p = 0.0010$ for D.

Signaling pathways involved in the $A\beta_{1\text{-}42}$ effects on glial cortical cultures

We studied the temporal profile activation of ERK 1/2 and AKT proteins at 10, 30, and 90 min after treating the WT and PK-KO glial cultures with 4.4 μM of $A\beta_{1\text{-}42}$. The levels of p-ERK (Fig. 5A) increased more in PK-KO glial cells after the treatment with $A\beta_{1\text{-}42}$ than in WT cultures. Similarly, there was a greater activation of p-AKT pathway at 10 and 30 min in PK-KO than in WT glial cells (Fig. 5B). There were no differences in basal levels of p-ERK or p-AKT between WT and PK-KO cultures.

Proteasome activity, ubiquitination, and autophagy in WT and PK-KO neuron-glia cortical cultures treated with $A\beta_{1\text{-}42}$

The $A\beta_{1\text{-}42}$, 4.4 μM treatment for 48 h, decreased the chymotrypsin- (Fig. 6A), trypsin- (Fig. 6B), and

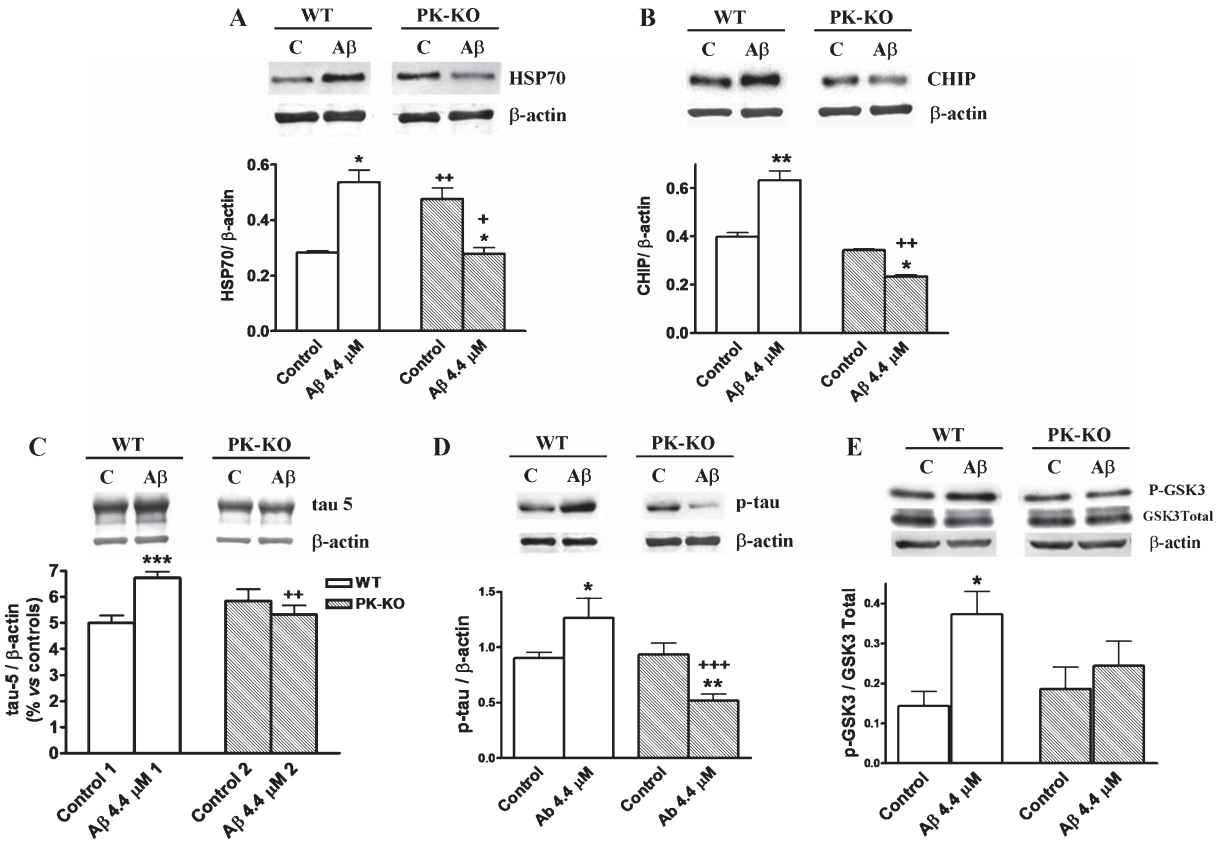

Fig. 4. Differential effects of oligomeric $A\beta_{1-42}$ on chaperones and tau proteins. At 5 DIV WT and PK-KO neuron-glia cultures were treated with $A\beta_{1-42}$ for 48 h. A) Representative western blot and densitometric analysis of HSP-70 and CHIP proteins (B) studied after 48 h of the Aβ peptide treatment. Total (C) and phosphorylated tau (D) proteins, expressed as Tau-5/ and AT-8/β-actin ratios after $A\beta_{1-42}$ treatment. Phosphorylated GSK3/total GSK3 ratios (E). β-actin was used as charge control. Values are the mean ± SEM from two independent experiments with 4 replicates each. Statistical analysis was performed by one or two-way ANOVA followed by Newman Keuls multiple comparison test and Bonferroni post-test, respectively. $^{*}p<0.05$, $^{**}p<0.01$, $^{***}p<0.001$ Aβ-treated cultures versus their respective controls; $^{+}p<0.05$, $^{++}p<0.01$, $^{+++}p<0.001$ PK-KO versus WT cultures. The interaction between the genotype and the treatment was $F(1,16)=50.71$; $p<0.0001$ for A. $F(1,10)=45.99$; $p<0.0001$ for B. $F(1,34)=12.06$; $p=0.0014$ for C and $F(1,32)=13.35$; $p=0.0009$ for D.

PGPH-like (Fig. 6C) activities of the proteasome in both WT and PK-KO mixed cortical cultures.

The ubiquitination state of total proteins, analyzed with an anti-ubiquitin antibody, was assessed in neuron-glia cortical cultures after treatment for 48 h with $A\beta_{1-42}$. The results (Fig. 6D, E) show that a global increase in polyubiquitinated proteins was only found in WT cells treated with the $A\beta_{1-42}$ peptide.

Next, we investigated how the treatment of WT and PK-KO neuron-glia cortical cultures with 4.4 μM of $A\beta_{1-42}$ modifies autophagy markers such as the protein microtubule-associated protein 1 light chain 3 (LC3), Beclin 1, and P62 protein. Thus, the $A\beta_{1-42}$, 4.4 μM treatment for 48 h caused a significant shift in the LC3-II/LC3-I and LC3-II/β-actin ratios (Fig. 6F), indicating an increase of autophagosomes in PK-KO but not in WT cultures. The percentage of P62 protein (Fig. 6G) did not change in WT Aβ peptide-treated cultures but it was significantly decreased in PK-KO-treated cultures. We did not observed changes in Beclin 1 protein in WT or PK-KO-treated cultures (Fig. 6H).

In order to obtain a direct evidence for upregulation of CMA in PK-KO cells, we analyzed the expression of LAMP-2A and HSC70 proteins levels, as well as the percentage of double LAMP-2A/HSC70 positive cells in the four experimental groups (Fig. 7). The percentage of cells immunoreactive to both HSC70 and LAMP-2A increased in PK-KO cultures versus WT and in PK-KO cultures treated with $A\beta_{1-42}$ (Fig. 7A, B). In addition, HSC70/LAMP-2A relocates to the perinuclear region in PK-KO cultures treated with $A\beta_{1-42}$ (Fig. 7E). Furthermore, LAMP-2A and HSC70 proteins levels increased in PK-KO cultures treated with $A\beta_{1-42}$ (Fig. 7C, D).

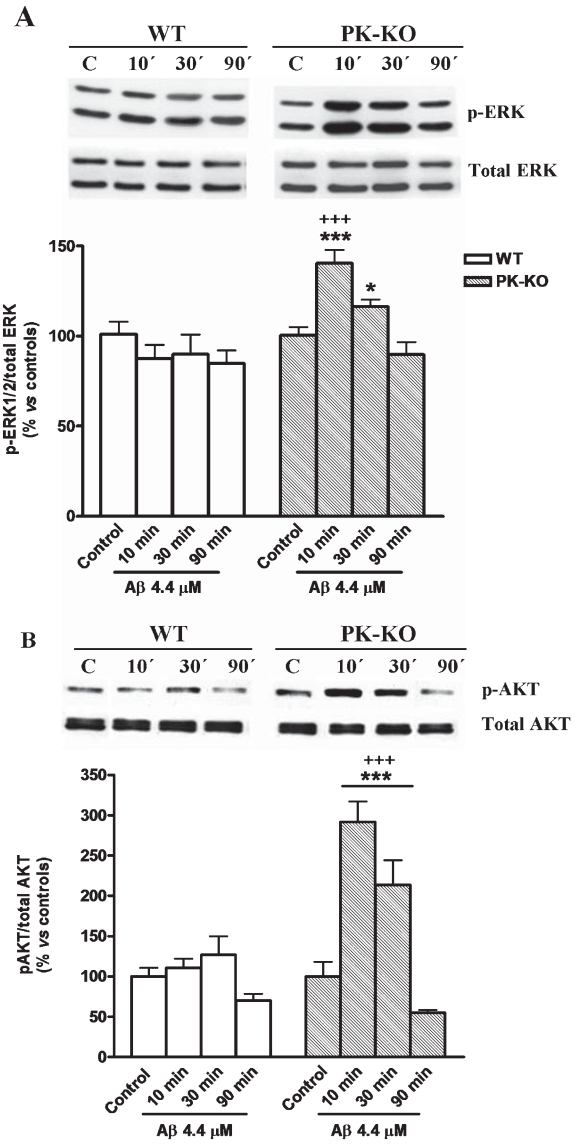

Fig. 5. Signaling pathways involved in the oligomeric $A\beta_{1\text{-}42}$ effects in WT and PK-KO cortical glial cultures. 6-7 days after reseeding glial cultures the medium was changed to defined medium and then treated with $A\beta_{1\text{-}42}$ (4.4 μM) for different periods of time. A) Western blot and densitometric analysis showing the time course activation of p-ERK 1/2 in WT and PK-KO glial cultures treated with $A\beta_{1\text{-}42}$ for the indicated times. B) Western blot and densitometric analysis showing AKT phosphorylation after 10, 30, and 90 min of $A\beta_{1\text{-}42}$ treatment. Values are the mean ± SEM from two independent experiments with 4 replicates each. Statistical analysis was performed by one or two-way ANOVA followed by Newman Keuls multiple comparison test and Bonferroni post-test, respectively. $^{*}p < 0.05$, $^{***}p < 0.001$ Aβ-treated cultures versus their respective controls; $^{+++}p < 0.001$ PK-KO versus WT cultures. The interaction between the genotype and the treatment was $F(3,47) = 12.76$; $p < 0.0001$ for B.

The inhibition of autophagy or GSH synthesis blocks the differential response of WT and PK-KO cultures to $A\beta_{1\text{-}42}$

To determine the role of autophagy in the differential response to $A\beta_{1\text{-}42}$ from WT and PK-KO cultures, we used the autophagy inhibitor 3-methyladenine at 0.5 mM [49], 30 min before the amyloid peptide treatment (4.4 μM for 48 h). PK-KO resistance to $A\beta_{1\text{-}42}$-induced cell death disappears with the 3-MA pre-treatment (Fig. 8A, B).

Previous studies have reported alterations in the GSH system in brain and peripheral cells of AD patients, as well as in several experimental models of AD [50–52]. So, we measured the intracellular levels of GSH after 48 h of incubation with 4.4 μM $A\beta_{1\text{-}42}$ or solvent. The GSH content decreases with the Aβ-treatment in WT, as shown in Fig. 8C, but not in PK-KO cultures. In addition, GPx activity and GR protein levels increased in PK-KO versus WT cultures, and furthermore in PK-KO cultures treated with $A\beta_{1\text{-}42}$ (supplementary Figure 4).

In order to determine if GSH homeostasis plays a key role in the differential response to $A\beta_{1\text{-}42}$ from WT and PK-KO cultures, we treated the cortical cultures with BSO (0.75 μM), an inhibitor of glutamylcysteine synthetase, which prevented *de novo* synthesis of GSH [49]. No cytotoxicity was observed in primary cortical WT and PK-KO cultures treated only with BSO. However, a significant increase in condensed nuclei, which are indicative of apoptotic cell death, was detected after the combined treatment of BSO and Aβ in both WT and PK-KO treated cells (Fig. 8D, E).

DISCUSSION

In this study, we found that PK-KO cortical cultures were more resistant than WT to the toxicity of $A\beta_{1\text{-}42}$. We have already shown than partial or complete suppression of parkin protects from amyloid pathology to mice with the AβPPswe mutation, but now we show that the neuroprotective effects of the lack of parkin takes also place in acute exposure to exogenous $A\beta_{1\text{-}42}$. We have also here investigated the mechanism of neuroprotection of the suppression of parkin on $A\beta_{1\text{-}42}$ toxicity and found that it is probably related, at least in part to a compensatory over production of GSH and an enhancement of autophagy.

$A\beta_{1\text{-}42}$ peptide induced significant cell death, increased astrogliosis, and microglial proliferation in

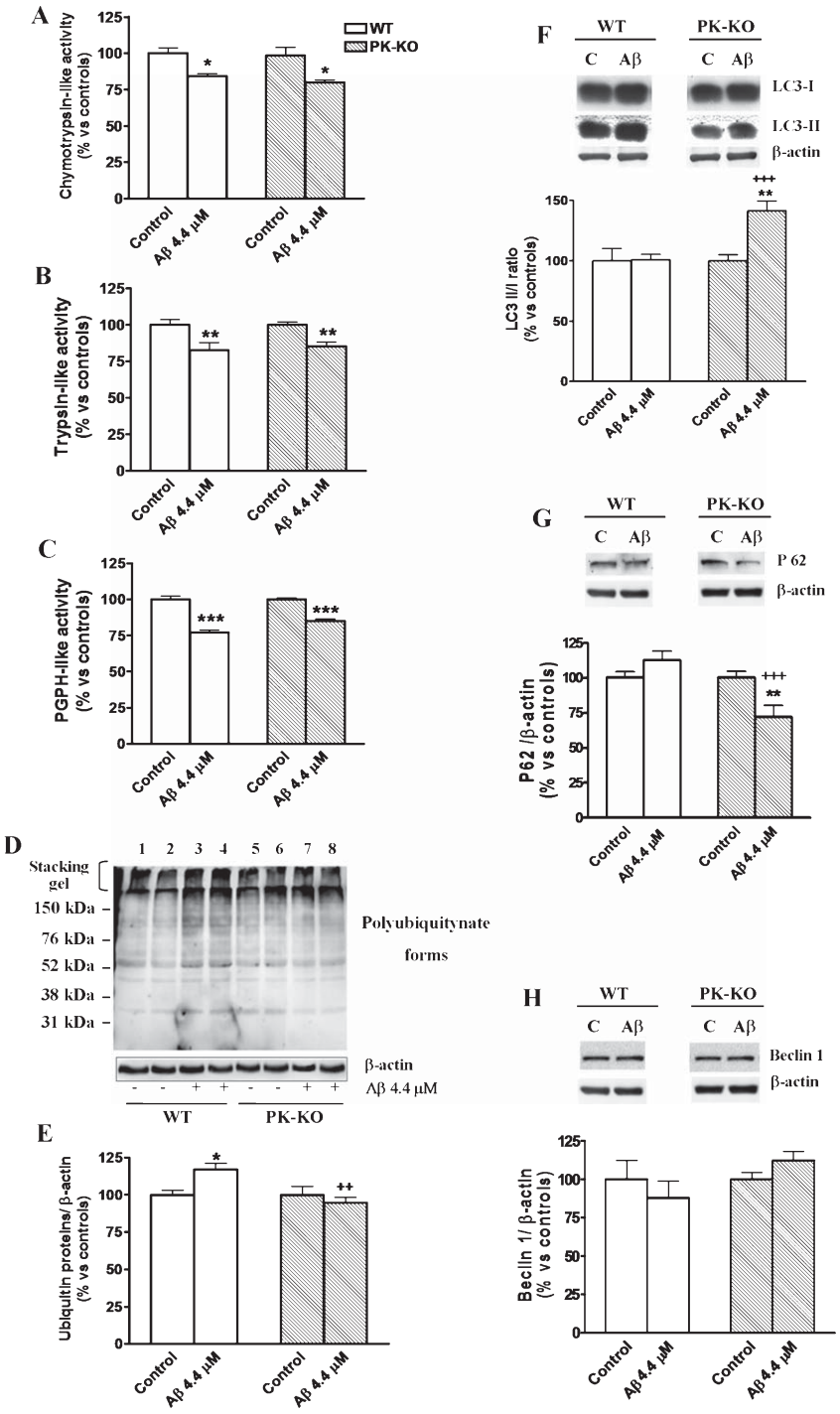

Fig. 6. Effects of $A\beta_{1\text{-}42}$ on proteasome activity, ubiquitination, and autophagy in WT and PK-KO neuron-glia cortical cultures. After 5 DIV, the cultures were treated with $A\beta_{1\text{-}42}$ (4.4 μM for 48 h) or solvent. A) Chymotrypsin-like, (B) Trypsin-like, and (C) peptidyl-glutamyl-peptide hydrolyzing (PGPH)-like proteasome activities in extracts prepared from WT and PK-KO neuron-glia cells. D) Accumulation of poly-ubiquitinated proteins and their corresponding densitometric analysis (E) after 48 h of $A\beta_{1\text{-}42}$ treatment. Western blot and densitometric analysis of LC3 (F), P62 (G), and Beclin 1 m(H) proteins in WT and PK-KO cultures. β-actin was used as charge control. Values are the mean ± SEM from two independent experiments with 4 replicates each. Statistical analysis was performed by one way ANOVA followed by Newman Keuls multiple comparison test. $^{*}p<0.05$, $^{**}p<0.01$, $^{***}p<0.001$ Aβ-treated cultures versus their respective controls; $^{++}p<0.01$, $^{+++}p<0.001$ PK-KO versus WT cultures.

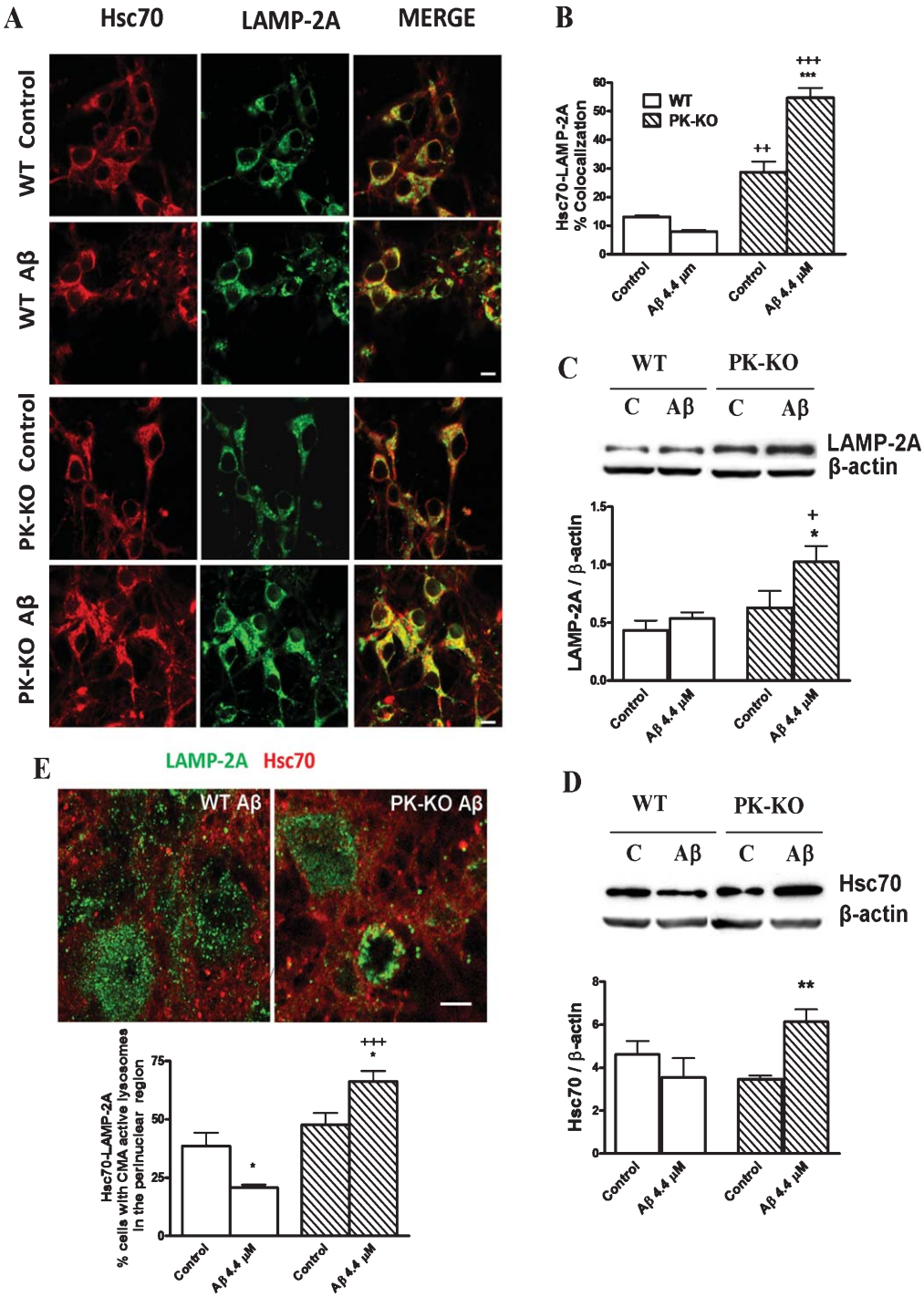

Fig. 7. HSC70 interacts with LAMP-2A in CMA Active Lysosomes; different response to $A\beta_{1\text{-}42}$ from WT and PK-KO cultures. A) Immunofluorescence for HSC70 and LAMP-2A cultures treated with Aβ for 48 h. B) Percentage of colocalization calculated in >25 cells ($n = 5$). Scale bar = 10 μm. C-D) Immunoblot for HSC70 and LAMP-2A proteins. β-Actin was used as an equal loading of proteins. E) Distribution of the LAMP-2A/HSC70-positive vesicles with respect to the nucleus, expressed as % cells with CMA active lysosomes (LAMP-2A/HSC70) in the perinuclear region. Scale bar, 10 μm. Values are the mean ± SEM from two independent cultures with 3–6 replicates each. Statistical analysis was performed by one or two-way ANOVA followed by Newman Keuls multiple comparison test and Bonferroni post-test, respectively. $^{*}p < 0.05$, $^{**}p < 0.01$, $^{***}p < 0.001$ Aβ treated PK-KO cultures versus their controls; $^{+}p < 0.05$, $^{++}p < 0.01$, $^{+++}p < 0.001$ PK-KO versus WT cultures. The interaction between the genotype and the treatment was $F(1,28) = 28{,}79$; $p < 0.0001$ for B and $F(1,24) = 34{,}25$; $p < 0.0001$ for E.

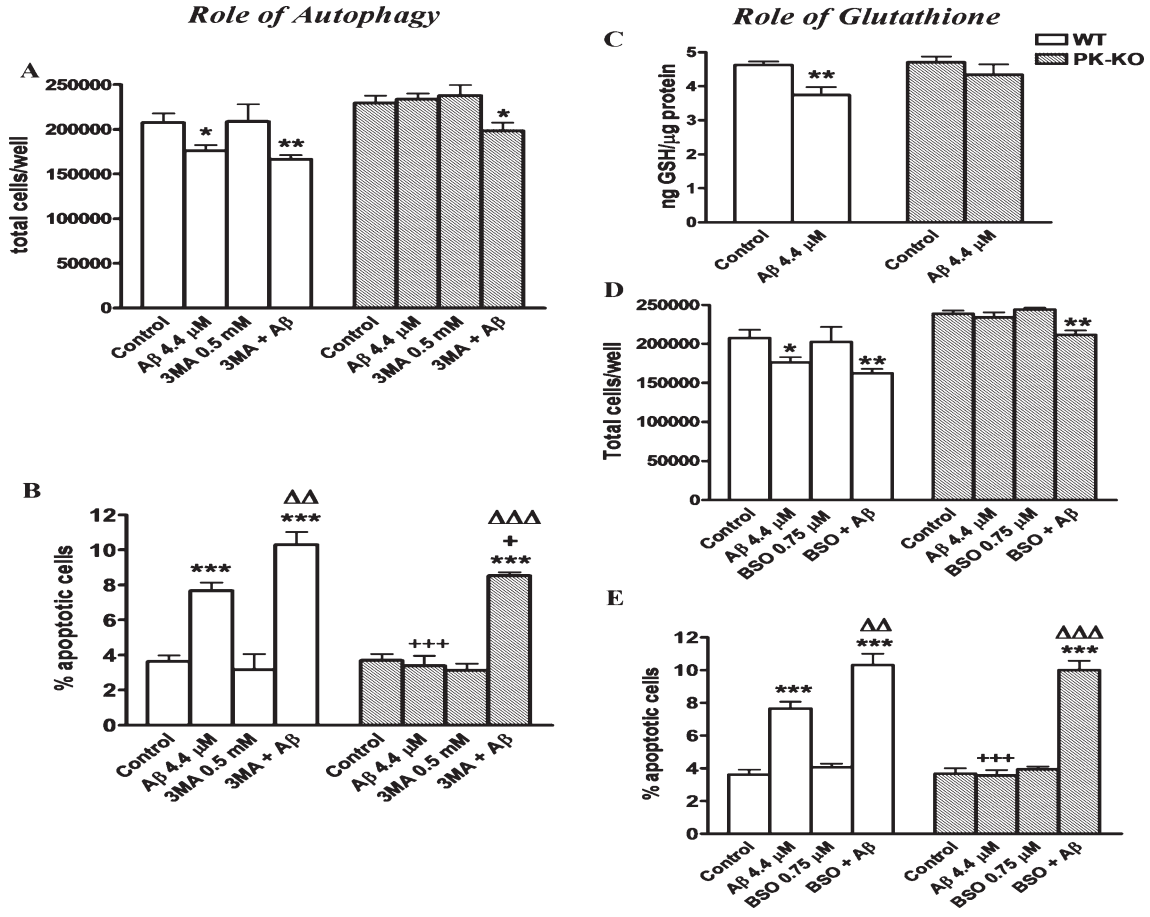

Fig. 8. Autophagy or GSH synthesis inhibition blocks the different response to $A\beta_{1\text{-}42}$ from WT and PK-KO cultures. After 5 DIV, WT and PK-KO mixed cultures were pre-treated with the autophagy inhibitor 3-methyladenine (3-MA) at 0.5 mM or BSO at 0.75 μM 30 min before $A\beta_{1\text{-}42}$ treatment (4.4 μM for 48 h). A, D) Number of total cells present in the different experimental groups. B, E) Chromatin condensed and fragmented nuclei were counted and expressed as a percentage of apoptotic cells with respect to the total cell number. C) GSH levels in WT and PK-KO cultures after $A\beta_{1\text{-}42}$ treatment. Values are the mean ± SEM from one representative experiment with 6 replicates each. Statistical analysis was performed by one or two-way ANOVA followed by Newman Keuls multiple comparison test and Bonferroni post-test, respectively. $^{*}p<0.05$, $^{**}p<0.01$, $^{***}p<0.001$ Aβ-treated cultures versus their respective controls; $^{+}p<0.05$, $^{+++}p<0.001$ PK-KO versus WT cultures. $^{\Delta\Delta}p<0.01$, $^{\Delta\Delta\Delta}p<0.001$ versus the corresponding Aβ treatment without inhibitors. The interaction between the genotype and the treatment was $F(3,30)=9.81$; $p=0.0005$ for B and $F(3, 37)=14.44$; $p<0.0001$ for E.

mixed neuronal-glial WT cultures, but it is toxic for astrocytes in pure glial cultures. These findings are in agreement with the traditional clinical observation of proliferation of glia in cases of neuronal death and suggest that neuronal death triggers glial proliferation. These effects were associated with increased levels of cytochrome C and an increase of the levels of total and phosphorylated tau and the levels of chaperones HSP70 and CHIP. $A\beta_{1\text{-}42}$ peptide significantly reduced proteasomal activities in both WT and PK-KO cultures, but the ubiquitination state of cell proteins only increase in WT cultures. The increased resistance of PK-KO cultures is associated with pro-survival mechanisms, such as the short activation of ERK1/2 and AKT signaling pathways, the activation of macro-autophagy and chaperone mediated autophagy, and the increased production of free radical scavengers, such as GSH. The inhibition of GSH synthesis by BSO or autophagy by 3MA reverted the resistance of the PK-KO cultures to $A\beta_{1\text{-}42}$ toxicity.

Parkin is an ubiquitin ligase 3 whose mutations produce PD. Parkin is present in Lewy bodies [53–59] which contain aggregated α-synuclein, suggesting that parkin plays a role in the processing of abnormal α-synuclein. In addition, parkin regulates exocytosis of neurotransmitters and synaptic function. Parkin suppression produces an excess of free radicals in dopamine neurons [34], which eventually leads to

neuronal death. This excess of free radical is temporarily compensated in young parkin null animals by an increased production of GSH. But in aged parkin null animals, the levels of GSH drop below normal values and the number of dopamine neurons drop dramatically [37, 60].

Parkin plays a key role in the interaction with different proteins. In the double mutants $PK^{-/-}/Tau^{VLW}$, Parkin deletion causes cerebral and systemic amyloidosis in human mutated over-expressing mice [6]. However, in the double mutant AβPPswe/Tau^{VLW}, Parkin suppression ameliorates amyloid and tau pathology and improves mice behavior and survival [6]. We showed in this study that the mechanisms on $A\beta_{1\text{-}42}$ toxicity are probably related to a compensatory over production of GSH and an enhancement of autophagy.

The role of parkin in the processing of abnormal proteins or cellular organelles is intriguing. Parkin, as E3 ubiquitin ligase reduces the levels of intracellular proteins by ubiquitination and proteasomal degradation [6, 8, 53, 61]. Parkin, acting through the ubiquitin proteosomal system and stimulating autophagy, ship off altered proteins and mitochondria [33, 62]. With respect to the interaction between parkin and $A\beta_{1\text{-}42}$ peptide, Burns and colleagues [6] showed that parkin promotes the clearance of intracellular $A\beta_{1\text{-}42}$, via UPS in M17 neuroblastoma cells over-expressing human parkin. Furthermore, Khandelwal and collaborators [7] showed that parkin mediated Beclin dependent autophagic clearance of defective mitochondria and ubiquitinated $A\beta_{1\text{-}42}$ peptide in a triple transgenic mice model of AD. All these findings predicted an aggravation of the $A\beta_{1\text{-}42}$ toxicity in parkin null neuronal cultures.

Parkin promotes ubiquitination and proteasomal degradation of intracellular $A\beta_{1\text{-}42}$ and demonstrates a protective effect in neurodegenerative diseases with Aβ deposits [6]. Parkin is cytoprotective, partially by increasing the removal of cellular Aβ through a proteasome-dependent pathway [6]. However, when Parkin is knocked out, autophagy may increases as a compensatory mechanism.

The process of autophagy, however, is complex and it has at least three inter-related mechanisms: proteasome mediated autophagy (PMA), chaperone mediated autophagy (CMA), and macroautophagy. There is evidence for different type profile of activation of these mechanisms and for complementary activation of one of these systems when the other is impairs [43, 63–65]. In autophagy triggered by fasting, for instance, macroautophagy is short lasting and takes place during the very first hours, while CMA starts later and is more prolonged. We assume that our parkin null neurons have impaired PMA and macroautophagy and a compensatory activation of CMA which allows for a more efficient degradation of $A\beta_{1\text{-}42}$ peptides. We demonstrated in this study that CMA is increased in PK-KO cortical cultures and furthermore in PK-KO cultures treated with $A\beta_{1\text{-}42}$.

Parkin null cortical cultures resistance to $A\beta_{1\text{-}42}$ disappears with the blockade of GSH synthesis or CMA. These findings support the relation of CMA with oxidative stress [66]. GSH homeostasis is critical for the survival of parkin null cultures and their resistance to several neurotoxins [36, 49, 67]. On the other hand, GSH may be neuroprotective for parkin null neurons via scavenging free radicals and facilitating CMA [49]. Perucho et al. [2] obtained similar results in double transgenic mice with the $A\beta PP_{swe}$ mutation and with parkin suppression.

The UPS is abnormal in AD [68–71] and its function is impaired by $A\beta_{1\text{-}42}$ peptides [8, 72, 73]. In this study we found that $A\beta_{1\text{-}42}$ treatment reduces the activities of the three proteosomal enzymes in WT and parkin null cultures. Autophagy is a compensatory mechanism to UPS dysfunction, essential for neuronal survival in aging and disease [74–78]. We found that the treatment with $A\beta_{1\text{-}42}$ peptide increased the levels of ubiquitin-protein conjugates in WT cells but decreased those in parkin null cells, suggesting that parkin null cell develop compensatory mechanisms for elimination of abnormal proteins. That explanation is supported by the finding of a shift of the autophagy marker, LC3-II/LC3-I ratio and a decrease in the percentage of P62 protein in parkin null cells treated with $A\beta_{1\text{-}42}$ peptide. The LC3 protein is anchored via conjugated phosphatidylethanolamine to the vesicle's membrane. While the un-conjugated LC3 is called LC3-I, the conjugated form is referred to as LC3-II, which is a specific marker for autophagosomes [79] and is degraded after fusion of autophagosomes with lysosomes [80]. P62 interacts with LC3 and functions as the cargo receptor for autophagy [81] and handles formation of cytoplasmic ubiquitin-positive inclusions [82]. Furthermore, P62 is itself a substrate of autophagy and is continuously degraded [83–85]. Beclin mediated autophagy, which clears defective mitochondria, was not altered in WT neither in parkin null neuronal cultures.

We found that $A\beta_{1\text{-}42}$ is toxic to cultured neurons, supporting the involvement of Aβ peptides in the neurodegeneration associated with AD [86–89]. In this study, $A\beta_{1\text{-}42}$ reduced the number of MAP-2^{+} neurons in cortical neuron-glia cultures from WT mice. The

percentage of astroglia and microglia was increased in $A\beta_{1-42}$-treated WT cultures. In contrast, administration of $A\beta_{1-42}$ to PK-KO cultures did not induce neuronal loss, astrogliosis or proliferation of microglia.

We also found that $A\beta_{1-42}$ increased the levels of cytochrome C in WT-treated cultures, but not in PK-KO. Cytochrome C release from mitochondria is an important step in apoptotic process and Aβ has been proved to induce cytochrome C release [90]. The treatment with $A\beta_{1-42}$ peptide increased of the levels of chaperones HSP70 and CHIP, in WT cultures, suggesting a compensatory response to the stress of the toxic peptide. HSP70 is a heat shock protein which responds to insults and stress and works as a chaperone refolding truncated proteins. CHIP is a 3-ubiquitin ligase that marks proteins to ubiquitin proteosomal system degradation. CHIP and HSP70 acts together as Aβ clearance promoters [91]. Magrane and colleagues [92] have shown that HSP70 is upregulated as part of the stress response to intracellular Aβ accumulation in cultured neurons. The transduction with HSP70 reduced $A\beta_{1-42}$-induced toxicity, suggesting that the endogenous stress response in neurons was insufficiently protective against Aβ treatment [92]. We observed that the baseline levels of HSP70 in parkin null cortical cultures were higher than those of WT cultures. Upregulation of HSP70 expression provides cytoprotection against Aβ peptides [93]. Heat shock proteins can neutralize the neurotoxicity in animal models suggesting potential therapeutic approaches in neurodegeneration associated with abnormal folding and toxicity [94, 95]. HSP70 increases with age in WT mice but not in PK-KO [60], and in aged glial cultures from both WT and PK-KO but more importantly in the former than in the latter [37]. In parkin null $A\beta_{1-42}$ treated cultures, the chaperones were reduced suggesting that CMA is very much activated and that the complex abnormal peptide-chaperone are internalized and degraded in the lysosomes.

Tau hyperphosphorylation and abnormal conformation is present in AD, and considered as a consequence of abnormal $A\beta_{1-42}$ peptide processing [96–99]. In this study, we confirm that $A\beta_{1-42}$ peptide increases the levels of tau and phospho-tau in WT cultures as it has been previously described [99–103] but reduced these levels in parkin null cultures. Tau accumulation and hyperphosphorylation takes place with inhibition of the proteasome [49, 104]. In parkin null mice, tau accumulation and hyperphosphorylation appear in aged animals, at the time when GSH levels are depleted and CMA impaired [60]. In this study, the reduction of total tau and hyperphosphorylated tau is compatible with the above mentioned enhancement of CMA and lysosomal processing of chaperone + tau complexes.

The ERK and AKT signaling pathways have important roles in neuronal function [74, 105–108]. Short activation of p-ERK1/2 is implicated in cell survival and long-activation in cell death [37, 38, 104]. In this study $A\beta_{1-42}$ treatment transiently increased the phosphorylation state of ERK and AKT proteins in parkin null but not in WT cells. The maximal activation takes place 10 min after incubation with $A\beta_{1-42}$. An extensive activation of ERK in astroglial cells was also observed in early stages of AD, whereas in advanced AD the phospho-ERK immunoreactivity was associated with neuronal cell bodies and dystrophic neurites around plaques [109]. AKT activation can be neuroprotective in several neurodegenerative disease models [110, 111]. For instance, activation of AKT kinase activity by insulin growth factor 1 (IGF-1) protected against mutant huntingtin-induced toxicity, and AKT was altered in Huntington's disease patients [112]. The relation between free radicals, activation of the signaling pathways, and autophagy only recently started to be investigated. Ablation of AKT induced macro autophagy through arrest of the cell cycle and deregulation of mitochondria [113]. With regards to ERK and autophagy there is evidence for a non canonical MEK/ERK pathway which modulates autophagy by regulating Beclin 1 [108]. More recent experiments have shown that free radicals activate another non-canonical mechanism of autophagy, which is independent of Beclin, as in our study, and mediated by activation JNK and ERK [114]. This last mechanism, which links free radical, activation of signaling pathways and CMA is probably very important in our study.

In conclusion, this study demonstrates that the treatment of cortical neuronal-glial cultures with $A\beta_{1-42}$ peptide produces different results according to the status of the different components of the autophagy system. In conditions such as parkin suppression, where there is impairment of the UPS and macroautophagy of abnormal cellular organelles, the compensatory activation of CMA could compensate the deficit and provide a neuroprotective effect against the toxic peptide. Thus, pharmacological stimulation of CMA could provide new neuroprotective approaches against neurodegenerative disorders.

ACKNOWLEDGMENTS

Supported in part by grants from the Comunidad de Madrid (Lain Entralgo NDG07/4 and

CAM S2011/BMD-2308), Spanish Ministry of Health, FIS 2007/PI07037, FIS 2010/172, CIBERNED 2006/05/0059, and CIBERNED PI2010-6. The authors thank Mrs. Mª Paz Muñoz for excellent technical assistance and Mrs. Claire Marsden for editorial help.

Authors' disclosures available online (http://www.j-alz.com/disclosures/view.php?id=1343).

REFERENCES

[1] Rodriguez-Navarro JA, Gomez A, Rodal I, Perucho J, Martinez A, Furio V, Ampuero I, Casarejos MJ, Solano RM, de Yebenes JG, Mena MA (2008) Parkin deletion causes cerebral and systemic amyloidosis in human mutated tau over-expressing mice. *Hum Mol Genet* **17**, 3128-3143.

[2] Perucho J, Casarejos MJ, Rubio I, Rodriguez-Navarro JA, Gomez A, Ampuero I, Rodal I, Solano RM, Carro E, Garcia de Yebenes J, Mena MA (2010) The effects of parkin suppression on the behaviour, amyloid processing, and cell survival in APP mutant transgenic mice. *Exp Neurol* **221**, 54-67.

[3] Tanzi RE, Bertram L (2005) Twenty years of the Alzheimer's disease amyloid hypothesis: A genetic perspective. *Cell* **120**, 545-555.

[4] De Strooper B, Saftig P, Craessaerts K, Vanderstichele H, Guhde G, Annaert W, Von Figura K, Van Leuven F (1998) Deficiency of presenilin-1 inhibits the normal cleavage of amyloid precursor protein. *Nature* **391**, 387-390.

[5] Shen J, Kelleher RJ 3rd (2007) The presenilin hypothesis of Alzheimer's disease: Evidence for a loss-of-function pathogenic mechanism. *Proc Natl Acad Sci U S A* **104**, 403-409.

[6] Burns MP, Zhang L, Rebeck GW, Querfurth HW, Moussa CE (2009) Parkin promotes intracellular Abeta1-42 clearance. *Hum Mol Genet* **18**, 3206-3216.

[7] Khandelwal PJ, Herman AM, Hoe HS, Rebeck GW, Moussa CE (2011) Parkin mediates beclin-dependent autophagic clearance of defective mitochondria and ubiquitinated A{beta} in AD models. *Hum Mol Genet* **20**, 2091-2102.

[8] Rosen KM, Moussa CE, Lee HK, Kumar P, Kitada T, Qin G, Fu Q, Querfurth HW (2010) Parkin reverses intracellular beta-amyloid accumulation and its negative effects on proteasome function. *J Neurosci Res* **88**, 167-178.

[9] Puglielli L, Tanzi RE, Kovacs DM (2003) Alzheimer's disease: The cholesterol connection. *Nat Neurosci* **6**, 345-351.

[10] Reitz C, Tang MX, Schupf N, Manly JJ, Mayeux R, Luchsinger JA (2010) Association of higher levels of high-density lipoprotein cholesterol in elderly individuals and lower risk of late-onset Alzheimer disease. *Arch Neurol* **67**, 1491-1497.

[11] Simons M, Keller P, De Strooper B, Beyreuther K, Dotti CG, Simons K (1998) Cholesterol depletion inhibits the generation of beta-amyloid in hippocampal neurons. *Proc Natl Acad Sci U S A* **95**, 6460-6464.

[12] Wood WG, Schroeder F, Igbavboa U, Avdulov NA, Chochina SV (2002) Brain membrane cholesterol domains, aging and amyloid beta-peptides. *Neurobiol Aging* **23**, 685-694.

[13] Martins IJ, Berger T, Sharman MJ, Verdile G, Fuller SJ, Martins RN (2009) Cholesterol metabolism and transport in the pathogenesis of Alzheimer's disease. *J Neurochem* **111**, 1275-1308.

[14] Reiss AB, Wirkowski E (2009) Statins in neurological disorders: Mechanisms and therapeutic value. *ScientificWorldJournal* **9**, 1242-1259.

[15] Serrano-Pozo A, Vega GL, Lutjohann D, Locascio JJ, Tennis MK, Deng A, Atri A, Hyman BT, Irizarry MC, Growdon JH (2010) Effects of simvastatin on cholesterol metabolism and Alzheimer disease biomarkers. *Alzheimer Dis Assoc Disord* **24**, 220-226.

[16] Tamboli IY, Barth E, Christian L, Siepmann M, Kumar S, Singh S, Tolksdorf K, Heneka MT, Lutjohann D, Wunderlich P, Walter J (2010) Statins promote the degradation of extracellular amyloid {beta}-peptide by microglia via stimulation of exosome-associated insulin-degrading enzyme (IDE) secretion. *J Biol Chem* **285**, 37405-37414.

[17] Gough M, Parr-Sturgess C, Parkin E (2011) Zinc metalloproteinases and amyloid beta-peptide metabolism: The positive side of proteolysis in Alzheimer's disease. *Biochem Res Int* **2011**, 721463.

[18] Perucho J, Casarejos MJ, Gomez A, Solano RM, de Yebenes G, Mena MA (2012) Trehalose protects from aggravation of amyloid pathology induced by isoflurane anesthesia in APP(swe) mutant mice. *Curr Alzheimer Res* **9**, 334-343.

[19] Grimmer T, Tholen S, Yousefi BH, Alexopoulos P, Forschler A, Forstl H, Henriksen G, Klunk WE, Mathis CA, Perneczky R, Sorg C, Kurz A, Drzezga A (2010) Progression of cerebral amyloid load is associated with the apolipoprotein E epsilon4 genotype in Alzheimer's disease. *Biol Psychiatry* **68**, 879-884.

[20] Popp J, Lewczuk P, Frommann I, Kolsch H, Kornhuber J, Maier W, Jessen F (2010) Cerebrospinal fluid markers for Alzheimer's disease over the lifespan: Effects of age and the APOEepsilon4 genotype. *J Alzheimers Dis* **22**, 459-468.

[21] Zhong N, Weisgraber KH (2009) Understanding the association of apolipoprotein E4 with Alzheimer disease: Clues from its structure. *J Biol Chem* **284**, 6027-6031.

[22] Ono K, Condron MM, Teplow DB (2009) Structure-neurotoxicity relationships of amyloid beta-protein oligomers. *Proc Natl Acad Sci U S A* **106**, 14745-14750.

[23] Ono K, Yamada M (2011) Low-n oligomers as therapeutic targets of Alzheimer's disease. *J Neurochem* **117**, 19-28.

[24] Prado MA, Baron G (2012) Seeding plaques in Alzheimer's disease. *J Neurochem* **120**, 641-643.

[25] Rosen RF, Fritz JJ, Dooyema J, Cintron AF, Hamaguchi T, Lah JJ, Levine H 3rd, Jucker M, Walker LC (2012) Exogenous seeding of cerebral beta-amyloid deposition in betaAPP-transgenic rats. *J Neurochem* **120**, 660-666.

[26] Cookson MR (2005) The biochemistry of Parkinson's disease. *Annu Rev Biochem* **74**, 29-52.

[27] Imai Y, Soda M, Takahashi R (2000) Parkin suppresses unfolded protein stress-induced cell death through its E3 ubiquitin-protein ligase activity. *J Biol Chem* **275**, 35661-35664.

[28] Shimura H, Hattori N, Kubo S, Mizuno Y, Asakawa S, Minoshima S, Shimizu N, Iwai K, Chiba T, Tanaka K, Suzuki T (2000) Familial Parkinson disease gene product, parkin, is a ubiquitin-protein ligase. *Nat Genet* **25**, 302-305.

[29] Xiong H, Wang D, Chen L, Choo YS, Ma H, Tang C, Xia K, Jiang W, Ronai Z, Zhuang X, Zhang Z (2009) Parkin, PINK1, and DJ-1 form a ubiquitin E3 ligase complex promoting unfolded protein degradation. *J Clin Invest* **119**, 650-660.

[30] Zhang Y, Gao J, Chung KK, Huang H, Dawson VL, Dawson TM (2000) Parkin functions as an E2-dependent ubiquitin-protein ligase and promotes the degradation of the synaptic

vesicle-associated protein, CDCrel-1. *Proc Natl Acad Sci U S A* **97**, 13354-13359.

[31] Chan NC, Salazar AM, Pham AH, Sweredoski MJ, Kolawa NJ, Graham RL, Hess S, Chan DC (2011) Broad activation of the ubiquitin-proteasome system by Parkin is critical for mitophagy. *Hum Mol Genet* **20**, 1726-1737.

[32] Herman AM, Moussa CE (2011) The ubiquitin ligase parkin modulates the execution of autophagy. *Autophagy* **7**, 919-921.

[33] Yoshii SR, Kishi C, Ishihara N, Mizushima N (2011) Parkin mediates proteasome-dependent protein degradation and rupture of the outer mitochondrial membrane. *J Biol Chem* **286**, 19630-19640.

[34] Itier JM, Ibanez P, Mena MA, Abbas N, Cohen-Salmon C, Bohme GA, Laville M, Pratt J, Corti O, Pradier L, Ret G, Joubert C, Periquet M, Araujo F, Negroni J, Casarejos MJ, Canals S, Solano R, Serrano A, Gallego E, Sanchez M, Denefle P, Benavides J, Tremp G, Rooney TA, Brice A, Garcia de Yebenes J (2003) Parkin gene inactivation alters behaviour and dopamine neurotransmission in the mouse. *Hum Mol Genet* **12**, 2277-2291.

[35] Casarejos MJ, Menendez J, Solano RM, Rodriguez-Navarro JA, Garcia de Yebenes J, Mena MA (2006) Susceptibility to rotenone is increased in neurons from parkin null mice and is reduced by minocycline. *J Neurochem* **97**, 934-946.

[36] Casarejos MJ, Solano RM, Menendez J, Rodriguez-Navarro JA, Correa C, Garcia de Yebenes J, Mena MA (2005) Differential effects of l-DOPA on monoamine metabolism, cell survival and glutathione production in midbrain neuronal-enriched cultures from parkin knockout and wild-type mice. *J Neurochem* **94**, 1005-1014.

[37] Solano RM, Casarejos MJ, Menendez-Cuervo J, Rodriguez-Navarro JA, Garcia de Yebenes J, Mena MA (2008) Glial dysfunction in parkin null mice: Effects of aging. *J Neurosci* **28**, 598-611.

[38] Canals S, Casarejos MJ, de Bernardo S, Solano RM, Mena MA (2003) Selective and persistent activation of extracellular signal-regulated protein kinase by nitric oxide in glial cells induces neuronal degeneration in glutathione-depleted midbrain cultures. *Mol Cell Neurosci* **24**, 1012-1026.

[39] Hilwig I, Gropp A (1975) pH-dpendent fluorescence of DNA and RNA in cytologic staining with ″33258″ Hoeschst. *Exp Cell Res* **91**, 457-460.

[40] Pardo B, Paino CL, Casarejos MJ, Mena MA (1997) Neuronal-enriched cultures from embryonic rat ventral mesencephalon for pharmacological studies of dopamine neurons. *Brain Res Brain Res Protoc* **1**, 127-132.

[41] Ashwell K (1991) The distribution of microglia and cell death in the fetal rat forebrain. *Brain Res Dev Brain Res* **58**, 1-12.

[42] Streit WJ, Kreutzberg GW (1987) Lectin binding by resting and reactive microglia. *J Neurocytol* **16**, 249-260.

[43] Kaushik S, Cuervo AM (2008) Chaperone-mediated autophagy. *Methods Mol Biol* **445**, 227-244.

[44] Bandyopadhyay U, Sridhar S, Kaushik S, Kiffin R, Cuervo AM (2010) Identification of regulators of chaperone-mediated autophagy. *Mol Cell* **39**, 535-547.

[45] Tietze F (1969) Enzymic method for quantitative determination of nanogram amounts of total and oxidized glutathione: Applications to mammalian blood and other tissues. *Anal Biochem* **27**, 502-522.

[46] Flohe L, Gunzler WA (1984) Assays of glutathione peroxidase. *Methods Enzymol* **105**, 114-121.

[47] Haass C, Selkoe DJ (2007) Soluble protein oligomers in neurodegeneration: Lessons from the Alzheimer's amyloid beta-peptide. *Nat Rev Mol Cell Biol* **8**, 101-112.

[48] Iqbal K, Grundke-Iqbal I (2006) Discoveries of tau, abnormally hyperphosphorylated tau and others of neurofibrillary degeneration: A personal historical perspective. *J Alzheimers Dis* **9**, 219-242.

[49] Casarejos MJ, Solano RM, Rodriguez-Navarro JA, Gomez A, Perucho J, Castano JG, Garcia de Yebenes J, Mena MA (2009) Parkin deficiency increases the resistance of midbrain neurons and glia to mild proteasome inhibition: The role of autophagy and glutathione homeostasis. *J Neurochem* **110**, 1523-1537.

[50] Aksenov MY, Markesbery WR (2001) Changes in thiol content and expression of glutathione redox system genes in the hippocampus and cerebellum in Alzheimer's disease. *Neurosci Lett* **302**, 141-145.

[51] Casado A, Encarnacion Lopez-Fernandez M, Concepcion Casado M, de La Torre R (2008) Lipid peroxidation and antioxidant enzyme activities in vascular and Alzheimer dementias. *Neurochem Res* **33**, 450-458.

[52] Resende R, Moreira PI, Proenca T, Deshpande A, Busciglio J, Pereira C, Oliveira CR (2008) Brain oxidative stress in a triple-transgenic mouse model of Alzheimer disease. *Free Radic Biol Med* **44**, 2051-2057.

[53] Shimura H, Schlossmacher MG, Hattori N, Frosch MP, Trockenbacher A, Schneider R, Mizuno Y, Kosik KS, Selkoe DJ (2001) Ubiquitination of a new form of alpha-synuclein by parkin from human brain: Implications for Parkinson's disease. *Science* **293**, 263-269.

[54] Schlossmacher MG, Frosch MP, Gai WP, Medina M, Sharma N, Forno L, Ochiishi T, Shimura H, Sharon R, Hattori N, Langston JW, Mizuno Y, Hyman BT, Selkoe DJ, Kosik KS (2002) Parkin localizes to the Lewy bodies of Parkinson disease and dementia with Lewy bodies. *Am J Pathol* **160**, 1655-1667.

[55] Klein C, Schlossmacher MG (2007) Parkinson disease, 10 years after its genetic revolution: Multiple clues to a complex disorder. *Neurology* **69**, 2093-2104.

[56] Takao M, Ghetti B, Yoshida H, Piccardo P, Narain Y, Murrell JR, Vidal R, Glazier BS, Jakes R, Tsutsui M, Spillantini MG, Crowther RA, Goedert M, Koto A (2004) Early-onset dementia with Lewy bodies. *Brain Pathol* **14**, 137-147.

[57] Beyer K, Domingo-Sabat M, Humbert J, Carrato C, Ferrer I, Ariza A (2008) Differential expression of alpha-synuclein, parkin, and synphilin-1 isoforms in Lewy body disease. *Neurogenetics* **9**, 163-172.

[58] Humbert J, Beyer K, Carrato C, Mate JL, Ferrer I, Ariza A (2007) Parkin and synphilin-1 isoform expression changes in Lewy body diseases. *Neurobiol Dis* **26**, 681-687.

[59] Benbunan BR, Korczyn AD, Giladi N (2004) Parkin mutation associated parkinsonism and cognitive decline, comparison to early onset Parkinson's disease. *J Neural Transm* **111**, 47-57.

[60] Rodriguez-Navarro JA, Casarejos MJ, Menendez J, Solano RM, Rodal I, Gomez A, Yebenes JG, Mena MA (2007) Mortality, oxidative stress and tau accumulation during ageing in parkin null mice. *J Neurochem* **103**, 98-114.

[61] Khandelwal PJ, Moussa C (2010) The relationship between parkin and protein aggregation in neurodegenerative diseases. *Front Psychiatry* **2**, 12.

[62] Chan NC, Chan DC (2011) Parkin uses the UPS to ship off dysfunctional mitochondria. *Autophagy* **7**, 771-772.

[63] Bejarano E, Cuervo AM (2010) Chaperone-mediated autophagy. *Proc Am Thorac Soc* **7**, 29-39.

[64] Massey AC, Kaushik S, Sovak G, Kiffin R, Cuervo AM (2006) Consequences of the selective blockage of chaperone-mediated autophagy. *Proc Natl Acad Sci U S A* **103**, 5805-5810.

[65] Cuervo AM, Knecht E, Terlecky SR, Dice JF (1995) Activation of a selective pathway of lysosomal proteolysis in rat liver by prolonged starvation. *Am J Physiol* **269**, C1200-C1208.

[66] Kiffin R, Christian C, Knecht E, Cuervo AM (2004) Activation of chaperone-mediated autophagy during oxidative stress. *Mol Biol Cell* **15**, 4829-4840.

[67] Solano RM, Menendez J, Casarejos MJ, Rodriguez-Navarro JA, Garcia de Yebenes J, Mena MA (2006) Midbrain neuronal cultures from parkin mutant mice are resistant to nitric oxide-induced toxicity. *Neuropharmacology* **51**, 327-340.

[68] Alves-Rodrigues A, Gregori L, Figueiredo-Pereira ME (1998) Ubiquitin, cellular inclusions and their role in neurodegeneration. *Trends Neurosci* **21**, 516-520.

[69] Cecarini V, Ding Q, Keller JN (2007) Oxidative inactivation of the proteasome in Alzheimer's disease. *Free Radic Res* **41**, 673-680.

[70] Keck S, Nitsch R, Grune T, Ullrich O (2003) Proteasome inhibition by paired helical filament-tau in brains of patients with Alzheimer's disease. *J Neurochem* **85**, 115-122.

[71] Keller JN, Hanni KB, Markesbery WR (2000) Impaired proteasome function in Alzheimer's disease. *J Neurochem* **75**, 436-439.

[72] Tseng BP, Green KN, Chan JL, Blurton-Jones M, LaFerla FM (2008) Abeta inhibits the proteasome and enhances amyloid and tau accumulation. *Neurobiol Aging* **29**, 1607-1618.

[73] Zhao X, Yang J (2010) Amyloid-beta peptide is a substrate of the human 20S proteasome. *ACS Chem Neurosci* **1**, 655-660.

[74] Wong E, Cuervo AM (2010) Autophagy gone awry in neurodegenerative diseases. *Nat Neurosci* **13**, 805-811.

[75] Matsuda N, Tanaka K (2010) Does impairment of the ubiquitin-proteasome system or the autophagy-lysosome pathway predispose individuals to neurodegenerative disorders such as Parkinson's disease? *J Alzheimers Dis* **19**, 1-9.

[76] Korolchuk VI, Menzies FM, Rubinsztein DC (2009) A novel link between autophagy and the ubiquitin-proteasome system. *Autophagy* **5**, 862-863.

[77] Rubinsztein DC (2007) Autophagy induction rescues toxicity mediated by proteasome inhibition. *Neuron* **54**, 854-856.

[78] Yue Z, Friedman L, Komatsu M, Tanaka K (2009) The cellular pathways of neuronal autophagy and their implication in neurodegenerative diseases. *Biochim Biophys Acta* **1793**, 1496-1507.

[79] Mizushima N, Yamamoto A, Matsui M, Yoshimori T, Ohsumi Y (2004) *In vivo* analysis of autophagy in response to nutrient starvation using transgenic mice expressing a fluorescent autophagosome marker. *Mol Biol Cell* **15**, 1101-1111.

[80] Kabeya Y, Mizushima N, Ueno T, Yamamoto A, Kirisako T, Noda T, Kominami E, Ohsumi Y, Yoshimori T (2000) LC3, a mammalian homologue of yeast Apg8p, is localized in autophagosome membranes after processing. *EMBO J* **19**, 5720-5728.

[81] Knaevelsrud H, Simonsen A (2010) Fighting disease by selective autophagy of aggregate-prone proteins. *FEBS Lett* **584**, 2635-2645.

[82] Komatsu M, Waguri S, Koike M, Sou YS, Ueno T, Hara T, Mizushima N, Iwata J, Ezaki J, Murata S, Hamazaki J, Nishito Y, Iemura S, Natsume T, Yanagawa T, Uwayama J, Warabi E, Yoshida H, Ishii T, Kobayashi A, Yamamoto M, Yue Z, Uchiyama Y, Kominami E, Tanaka K (2007) Homeostatic levels of p62 control cytoplasmic inclusion body formation in autophagy-deficient mice. *Cell* **131**, 1149-1163.

[83] Bjorkoy G, Lamark T, Brech A, Outzen H, Perander M, Overvatn A, Stenmark H, Johansen T (2005) p62/SQSTM1 forms protein aggregates degraded by autophagy and has a protective effect on huntingtin-induced cell death. *J Cell Biol* **171**, 603-614.

[84] Kirkin V, Lamark T, Sou YS, Bjorkoy G, Nunn JL, Bruun JA, Shvets E, McEwan DG, Clausen TH, Wild P, Bilusic I, Theurillat JP, Overvatn A, Ishii T, Elazar Z, Komatsu M, Dikic I, Johansen T (2009) A role for NBR1 in autophagosomal degradation of ubiquitinated substrates. *Mol Cell* **33**, 505-516.

[85] Pankiv S, Clausen TH, Lamark T, Brech A, Bruun JA, Outzen H, Overvatn A, Bjorkoy G, Johansen T (2007) p62/SQSTM1 binds directly to Atg8/LC3 to facilitate degradation of ubiquitinated protein aggregates by autophagy. *J Biol Chem* **282**, 24131-24145.

[86] Agostinho P, Oliveira CR (2003) Involvement of calcineurin in the neurotoxic effects induced by amyloid-beta and prion peptides. *Eur J Neurosci* **17**, 1189-1196.

[87] Celsi F, Svedberg M, Unger C, Cotman CW, Carri MT, Ottersen OP, Nordberg A, Torp R (2007) Beta-amyloid causes downregulation of calcineurin in neurons through induction of oxidative stress. *Neurobiol Dis* **26**, 342-352.

[88] Resende R, Ferreiro E, Pereira C, Resende de Oliveira C (2008) Neurotoxic effect of oligomeric and fibrillar species of amyloid-beta peptide 1-42: Involvement of endoplasmic reticulum calcium release in oligomer-induced cell death. *Neuroscience* **155**, 725-737.

[89] Resende R, Pereira C, Agostinho P, Vieira AP, Malva JO, Oliveira CR (2007) Susceptibility of hippocampal neurons to Abeta peptide toxicity is associated with perturbation of Ca2+ homeostasis. *Brain Res* **1143**, 11-21.

[90] Qiao H, Koya RC, Nakagawa K, Tanaka H, Fujita H, Takimoto M, Kuzumaki N (2005) Inhibition of Alzheimer's amyloid-beta peptide-induced reduction of mitochondrial membrane potential and neurotoxicity by gelsolin. *Neurobiol Aging* **26**, 849-855.

[91] Kumar P, Ambasta RK, Veereshwarayya V, Rosen KM, Kosik KS, Band H, Mestril R, Patterson C, Querfurth HW (2007) CHIP and HSPs interact with beta-APP in a proteasome-dependent manner and influence Abeta metabolism. *Hum Mol Genet* **16**, 848-864.

[92] Magrane J, Smith RC, Walsh K, Querfurth HW (2004) Heat shock protein 70 participates in the neuroprotective response to intracellularly expressed beta-amyloid in neurons. *J Neurosci* **24**, 1700-1706.

[93] Hoshino T, Murao N, Namba T, Takehara M, Adachi H, Katsuno M, Sobue G, Matsushima T, Suzuki T, Mizushima T (2011) Suppression of Alzheimer's disease-related phenotypes by expression of heat shock protein 70 in mice. *J Neurosci* **31**, 5225-5234.

[94] Cummings CJ, Sun Y, Opal P, Antalffy B, Mestril R, Orr HT, Dillmann WH, Zoghbi HY (2001) Over-expression of inducible HSP70 chaperone suppresses neuropathology and improves motor function in SCA1 mice. *Hum Mol Genet* **10**, 1511-1518.

[95] Warrick JM, Chan HY, Gray-Board GL, Chai Y, Paulson HL, Bonini NM (1999) Suppression of polyglutamine-mediated neurodegeneration in Drosophila by the molecular chaperone HSP70. *Nat Genet* **23**, 425-428.

[96] De Felice FG, Wu D, Lambert MP, Fernandez SJ, Velasco PT, Lacor PN, Bigio EH, Jerecic J, Acton PJ, Shughrue PJ, Chen-Dodson E, Kinney GG, Klein WL (2008) Alzheimer's disease-type neuronal tau hyperphosphorylation induced by A beta oligomers. *Neurobiol Aging* **29**, 1334-1347.

[97] Ma QL, Lim GP, Harris-White ME, Yang F, Ambegaokar SS, Ubeda OJ, Glabe CG, Teter B, Frautschy SA, Cole GM (2006) Antibodies against beta-amyloid reduce Abeta oligomers, glycogen synthase kinase-3beta activation and tau phosphorylation *in vivo* and *in vitro*. *J Neurosci Res* **83**, 374-384.

[98] Younkin SG (1995) Evidence that A beta 42 is the real culprit in Alzheimer's disease. *Ann Neurol* **37**, 287-288.

[99] Zheng WH, Bastianetto S, Mennicken F, Ma W, Kar S (2002) Amyloid beta peptide induces tau phosphorylation and loss of cholinergic neurons in rat primary septal cultures. *Neuroscience* **115**, 201-211.

[100] Alvarez G, Munoz-Montano JR, Satrustegui J, Avila J, Bogonez E, Diaz-Nido J (1999) Lithium protects cultured neurons against beta-amyloid-induced neurodegeneration. *FEBS Lett* **453**, 260-264.

[101] Le WD, Xie WJ, Kong R, Appel SH (1997) Beta-amyloid-induced neurotoxicity of a hybrid septal cell line associated with increased tau phosphorylation and expression of beta-amyloid precursor protein. *J Neurochem* **69**, 978-985.

[102] Shea TB, Prabhakar S, Ekinci FJ (1997) Beta-amyloid and ionophore A23187 evoke tau hyperphosphorylation by distinct intracellular pathways: Differential involvement of the calpain/protein kinase C system. *J Neurosci Res* **49**, 759-768.

[103] Busciglio J, Lorenzo A, Yeh J, Yankner BA (1995) beta-amyloid fibrils induce tau phosphorylation and loss of microtubule binding. *Neuron* **14**, 879-888.

[104] Casarejos MJ, Solano RM, Gomez A, Perucho J, de Yebenes JG, Mena MA (2011) The accumulation of neurotoxic proteins, induced by proteasome inhibition, is reverted by trehalose, an enhancer of autophagy, in human neuroblastoma cells. *Neurochem Int* **58**, 512-520.

[105] Yuan J, Yankner BA (2000) Apoptosis in the nervous system. *Nature* **407**, 802-809.

[106] Cagnol S, Chambard JC ERK and cell death: Mechanisms of ERK-induced cell death–apoptosis, autophagy and senescence. *FEBS J* **277**, 2-21.

[107] Fan QW, Weiss WA (2011) Autophagy and Akt promote survival in glioma. *Autophagy* **7**, 536-538.

[108] Wang J, Whiteman MW, Lian H, Wang G, Singh A, Huang D, Denmark T (2009) A non-canonical MEK/ERK signaling pathway regulates autophagy via regulating Beclin 1. *J Biol Chem* **284**, 21412-21424.

[109] Webster B, Hansen L, Adame A, Crews L, Torrance M, Thal L, Masliah E (2006) Astroglial activation of extracellular-regulated kinase in early stages of Alzheimer disease. *J Neuropathol Exp Neurol* **65**, 142-151.

[110] Kaspar BK, Llado J, Sherkat N, Rothstein JD, Gage FH (2003) Retrograde viral delivery of IGF-1 prolongs survival in a mouse ALS model. *Science* **301**, 839-842.

[111] Magrane J, Rosen KM, Smith RC, Walsh K, Gouras GK, Querfurth HW (2005) Intraneuronal beta-amyloid expression downregulates the Akt survival pathway and blunts the stress response. *J Neurosci* **25**, 10960-10969.

[112] Humbert S, Bryson EA, Cordelieres FP, Connors NC, Datta SR, Finkbeiner S, Greenberg ME, Saudou F (2002) The IGF-1/Akt pathway is neuroprotective in Huntington's disease and involves Huntingtin phosphorylation by Akt. *Dev Cell* **2**, 831-837.

[113] Santi SA, Lee H (2011) Ablation of Akt2 induces autophagy through cell cycle arrest, the downregulation of p70S6K, and the deregulation of mitochondria in MDA-MB231 cells. *PLoS One* **6**, e14614.

[114] Wong CH, Iskandar KB, Yadav SK, Hirpara JL, Loh T, Pervaiz S (2010) Simultaneous induction of non-canonical autophagy and apoptosis in cancer cells by ROS-dependent ERK and JNK activation. *PLoS One* **5**, e9996.